Audio Engineering Society

Convention Paper 6911

Presented at the 121st Convention
2006 October 5–8 San Francisco, CA, USA

An Important Aspect of Underhung Voice-Coils: A Technical Tribute to Ray Newman

Raymond J. Newman (deceased)[1], D. B. (Don) Keele, Jr.[2], David E. Carlson[3], Jim Long[4], Kent H. Frye[5], and Matthew S. Ruhlen[6]

[1] Electro-Voice Inc., Buchanan, MI, 49107 USA (As of 1992)

[2] Harman International Industries, Martinsville, IN, 46151 USA
DKeele@Harman.com

[3] Electro-Voice, Div. Telex Communications, Burnsville, MN, 55337 USA
DE.Carlson@US.Telex.com

[4] Electro-Voice, Div. Telex Communications, Burnsville, MN, 55337 USA
JJimLong@cs.com

[5] Gentex Corporation, Fire Protection Group, Zeeland, MI, 49464 USA
KFrye@Gentex.com

[6] Harman/Becker Automotive Systems, Martinsville, IN, 46151 USA
MRuhlen@HarmanBecker.com

ABSTRACT

In the1970s, Ray Newman while at Electro-Voice, single handedly and very successfully promoted the use of the then new concept of the Thiele/Small parameters and related design techniques for categorizing loudspeakers and systems to the loudspeaker industry. This paper posthumously recounts the contents of three significant Electro-Voice memos written in 1992 by Ray Newman concerning a comparison of overhung versus underhung loudspeaker motor assemblies. The information in the memos is still very relevant today. He proposed a comparison between the two assembly types assuming motors that had: 1. the same Xmax, 2. the same efficiency, 3. similar thermal behavior, and 4. the same voice coil. He calculated the required magnetic gap energy and discovered to his surprise that the magnet requirements actually went down dramatically when switching from an overhung to an underhung structure and depended only on the ratio between Xmax and the voice-coil length. This is in contrast with "common sense" that dictates that longer gaps mean larger magnets. He showed that for high-excursion motors, a switch could be made from a ferrite overhung structure to an equivalent high-energy neodymium underhung structure with little cost penalty. This paper recounts this early work and then presents motor predictions using a present-day magnetic FEM simulator. The results show that indeed, the magnetic energy required by an underhung motor is actually less than an overhung motor as long as the operating flux in the underhung motor's core is below the point where the core and fringe losses are comparable to its gap energy. Ray's original memos and notes will also be included as an appendix to the paper along with reminiscences from the paper's co-authors .

1. INTRODUCTION

This paper is based on a series of three memos written by Ray Newman while he was at Electro-Voice (EV) in 1992 titled "An Important Aspect of Underhung Voice-Coils" (Appendix 1). The memos dealt with the magnet requirements for overhung and underhung loudspeaker motor structures and claimed that that an underhung loudspeaker motor required less magnet than a more traditional overhung motor. This was quite contrary to traditional design opinion at the time that claimed that underhung structures require more magnet not less.

One of this paper's authors (Keele), ran across a copy of the memos when he rejoined EV in 1996 (Keele worked for EV the first time around between 1972 and 1976). Thinking that the memo's results were very significant, he kept a copy of the memos and thought it would be very worthwhile to do some serious investigation to determine if Newman's claims were correct. Newman retired from EV in 1993 and then passed away in 1996.

Keele subsequently thought the memos and their content would make a very good paper topic and talked to several current and past employees of EV to see if they would be interested in co-authoring a paper. After gaining permission from EV's higher ups to talk about what at the time was a series of confidential memos, this paper is a result of that collaboration.

Newman based his analysis on considering the magnetic energy stored in the motor's voice-coil gap. He showed that that an underhung motor actually required less magnet energy than an equivalent overhung motor by making four assumptions concerning the speakers and their magnet assemblies:

1. The motors have the same excursion (X_{max}),
2. the same efficiency (equal *Bl* products),
3. have similar thermal behavior, and
4. use the same voice coil.

He then derived the ratio of gap magnetic energies between the underhung and overhung structures and found to his surprise that the magnet requirements actually went down dramatically when switching from an overhung to an underhung structure and depended only on the ratio between Xmax and the voice-coil length.

The equation he revealed in the first of his three memos was (with slight changes of variables):

$$\frac{E_u}{E_o} = 1 - 4\left(\frac{X_{\max}}{K}\right)^2 = 1 - 4R^2 \quad (1)$$

Where,

E_u = Gap energy of underhung motor

E_o = Gap energy of overhung motor

X_{max} = geometric maximum excursion of driver

K = Voice coil length

$R = X_{max}/K$ = ratio of X_{max} to voice-coil length.

A plot of this equation is shown in the following figure.

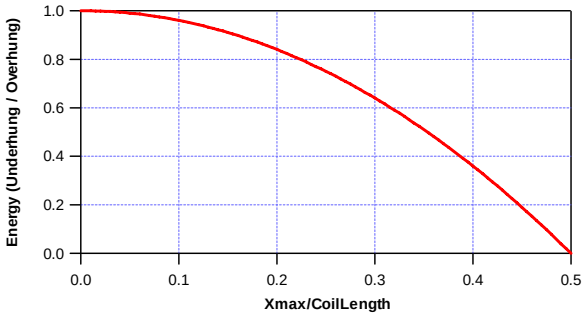

Fig. 1. Gap energy ratio comparing the underhung versus overhung magnetic structures according to the equation in Newman's first memo.

This rather surprising result indicates that the ratio of the energies actually falls dramatically as excursion is increased, and falls to zero when X_{max} is one-half the voice coil length ($Xmax/K$ = 0.5), i.e. the underhung structure seemingly requires no magnet at all! In Newman's first memo (Appendix 8.1) he has fun with this and claims that the derivation of Eq. 1 is "an exercise for the student" and that he will be glad to explain the "no magnet needed" case to anyone who is curious.

I (Keele) was successful in deriving Eq. 1 in Sept. 1996 but only understood the "no magnet needed" case when I started working on this paper!

This paper re-derives Eq. 1 in a somewhat round-about manner by first deriving equations for the normalized top-plate thickness, the normalized gap flux density, and the normalized gap energy for both the overhung and underhung structures. Normalization in this situation refers to quantities derived from a "so called" reference motor structure with an Xmax of zero, i.e. the top-plate thickness is equal to the voice-coil length (no overhang

or underhang). Once the normalized gap energies are calculated they are divided to form Eq. 1.

The unstated major assumption in the derivation of Newman's Eq. 1 was that the driver's magnetic losses in the motor's metal parts ("the core") and fringing was neglected.

The neglected magnetic losses are accounted for in the last part of this paper where several magnetic finite-element simulations are shown. The detailed simulations show that Newman was partially right in his claim that an underhung motor requires less magnet than an equivalent overhung motor when all driver losses are taken into account.

Simulations reveal that core losses in the underhung structure will tip the balance over to the overhung structure, but as long as the operating flux in the underhung structure's core is below the point where the underhung motor's core and fringe losses are comparable to its gap energy, that indeed less magnet energy is required for the underhung motor.

All three of Newman's memos are included in Appendix 1 of this paper.

Appendix 2 contains reminiscences of several co-authors of this paper.

In this paper, the thermal issues are ignored and only the magnetic issues are considered.

1.1. Ray Newman

The following information was gathered from AES author biographies and from Ray's wife, Mary (formerly Newman) Swider.

Raymond J. Newman was born in Wyandotte, Mich., in 1938. He received the B.S.E.E. degree from the University of Michigan in 1960. From 1960 to 1962 he was employed by the Aeronutronic Division of the Ford Motor Company (now Ford Aerospace) in Newport Beach, Calif., where he was responsible for the checkout and installation of instrumentation used on high-altitude research rockets and later for research and design tasks associated with the prediction and manipulation of electromagnetic fields scattered by arbitrary objects (radar cross-section analysis). From 1962 to 1967 he was employed by the Conduction Corporation of Ann Arbor, Michigan as a member of the Senior Analysis Staff, continuing his work in radar cross-section analysis.

From 1967 to the time of his retirement in the summer of 1993, Mr. Newman was with Electro Voice of Buchanan, Mich., serving in the capacity of Senior Engineer in charge of loudspeaker systems and later as chief engineer of loudspeakers. He was engaged in research, design, development of loudspeaker systems for commercial and home usage. Mr. Newman was a member of the Audio Engineering Society and the Institute of Electrical and Electronics Engineers. He is one of the authors of the book *Methods of Radar Cross-Section Analysis* published by Academic Press in 1968. Mr. Newman passed away on February 15, 1996.

In the early 1970's, Ray was one of the first engineers in the loudspeaker industry that saw the inherent worth in Nevile Thiele's and Richard Small's pioneering new research in applying analytical design techniques to loudspeakers and systems that had been published in the Journal of the Audio Engineering society [1-6].

Ray gave and published a number of papers on loudspeaker related topics [7-15] and wrote two magazine articles [16-17]. In 1972 he described the design of the first domestic loudspeaker based on one of Thiele's cabinet alignments, the "Interface A:" [8-9].

Neville Thiele was quoted in 2006 [18] saying:

"Then Dick (Small) wrote his series of publications, which you know about, for the Journal of the Audio Engineering Society, in 1972 and 1973, and had persuaded the Journal to reprint my 1961 paper in May and June of 1971. It was only then that people became interested in the Parameters. As far as I knew, Ray Newman and Don Keele at Electro-Voice were the first to use them."

1.2. Newman AES Journal Author Pictures

Fig. 2 shows three pictures of Ray Newman taken from the Journal of the Audio Engineering Society's "The Author" section dating from 1973 to 1989.

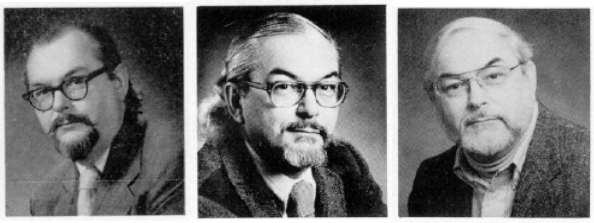

Fig. 2. AES journal "The Author" pictures of Ray Newman from the years 1973, 1980, and 1989 (left to right). Mr. Newman passed away on February 15, 1996 at the age of 58.

1.3. Newman's Memos on Underhung Voice-Coils

The three memos that Ray Newman wrote in 1993 that are the topic of this paper are shown in their entirety in Appendix 1. The memos themselves contain three handwritten appendices labeled X, Y, and Z along with Newman's handwritten notes from his engineering lab book that illustrate the concepts he was trying to convey.

2. AN IMPORTANT ASPECT OF UNDERHUNG VOICE-COILS

As stated in the introduction, this section re-derives Newman's Eq. 1 by first deriving equations for the normalized top-plate thickness, the normalized gap flux density, and the normalized gap energy for both the overhung and underhung structures. Normalization in this situation refers to quantities derived from a reference motor structure with an Xmax of zero, i.e. the top-plate thickness is equal to the voice-coil length (no overhang or underhang). Once the normalized gap energies are calculated they are then divided to form Eq. 1.

2.1. Derivation of Gap Energy Ratio Comparing Underhung vs. Overhung Motors

This section derives Newman's Eq. 1 that resulted in his graph shown in memos 1 and 2 (Appendix 1, Sections 8.1 and 8.2, and also shown here in Fig. 1) showing the ratio of underhung versus overhung gap energies.[1] This is essentially the follow through for what Newman suggests is an "exercise for the student" but in a somewhat round-about manner. The next subsections show a more detailed step-by-step derivation of the gap energy ratio relationships with intermediate steps showing the normalized top-plate thickness, normalized gap flux density, and the gap energies for both the overhung and underhung geometries.

2.1.1. Definition of Xmax

Newman's derivation of the gap magnetic energy ratio is based on a definition of the maximum excursion X_{max} that is equal to the so-called "geometric" maximum excursion where the coil just begins to leave the physical gap. This simplified version of X_{max} assumes linear operation in the range of $\pm X_{max}$, at which point the distortion may suddenly and dramatically increase for higher excursions. As Newman points out in his third memo (page 1, Appendix 1, Section 8.3), this geometric X_{max} is a bit restrictive because the coil can move some additional distance before the distortion becomes objectionable. Assuming this more restrictive value of maximum excursion, greatly simplifies the calculations of certain motor parameters in the derivations.

2.1.2. Maximum Excursions

Fig. 3 shows depictions of the overhung and underhung motor structures along with the mid, maximum up, and maximum down positions of the voice coil.

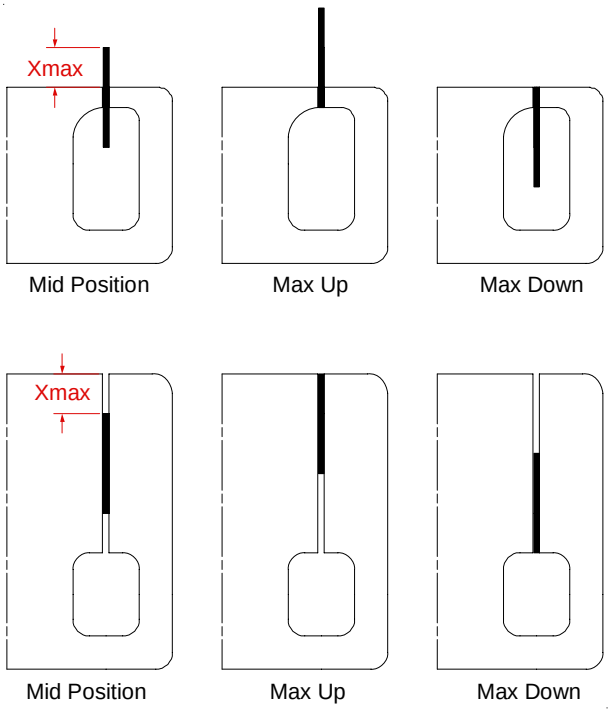

Fig. 3. Maximum voice-coil excursions for the overhung (top row) and underhung (bottom row) motor structures with the geometric X_{max} indicated. The drawings have the same scale as the structures used in the simulations of this paper with an X_{max} equal to 0.4 times the voice-coil length. Only the right half of the axially symmetric structure is shown. Mid position (left), maximum up position (middle), and maximum down position (right).

2.1.3. Motor Structures Analyzed

Fig. 4 shows depictions of the three motor structures analyzed.

[1] Interestingly, Matt Ruhlen, one of the co-authors of this paper, produced the graph shown in Ray's memos on his personal Apple Macintosh 512K computer.

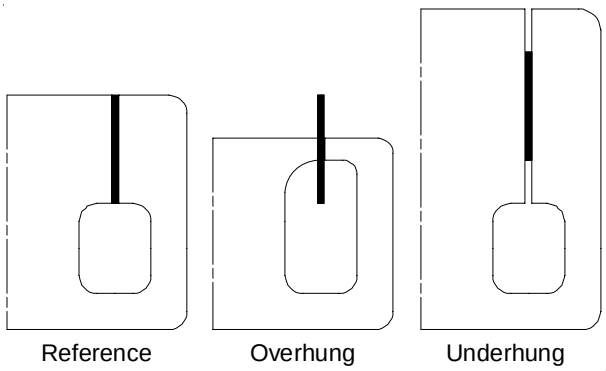

Fig. 4. Depictions of the three analyzed motor structures. Reference (left), overhung (middle), and underhung (right). The voice-coils are all shown in their mid position (long black rectangles). The drawings have the same scale as the structures used in the simulations of this paper with a geometric X_{max} equal to 0.4 times the voice-coil length for the middle and right structures and a geometric X_{max} of zero for the left structure (see Figs 8 -10 later). Only the right half of the axisymmetric structure is shown.

Reference Motor (X_{max} = 0)

The reference motor structure (Fig. 4 left) has a top-plate thickness equal to the voice-coil length. This structure is used as a reference for the normalizations.

Overhung Motor

The top-plate thickness of the overhung motor (Fig. 4 middle) is small in relation to the voice-coil length. The top plate thickness depicted here is 20% of the voice coil length.

Underhung Motor

The top-plate thickness of the overhung motor (Fig. 4 right) is longer than the voice coil by a factor of 1.8.

2.2. Normalized Top-Plate Thickness

Using simple geometric relationships, it can be shown that the top-plate thickness T_0 of an overhung motor can be written in terms of the voice-length K and the ratio R (= X_{max}/K) as follows:

$$T_O = K(1-2R) \qquad (2)$$

This can be normalized to the reference motor structure where X_{max} is zero by dividing both sides by K:

$$T_{ONorm} = \frac{T_O}{K} = 1-2R \qquad (3)$$

Likewise the normalized top-plate thickness of an underhung motor structure can be shown to be:

$$T_{UNorm} = \frac{T_U}{K} = 1+2R \qquad (4)$$

Plots of these two equations are shown in the following figure. This graph shows that as the structure's designed X_{max} increases, the overhung top-plate thickness decreases while the underhung top-plate thickness increases.

However, the overhung top-plate thickness can only shrink to zero to where X_{max} is equal to one-half the coil length, i.e. the coil can only move up or down a distance of one-half the coil length. Correspondingly, the underhung top-plate thickness doubles over the same range to be equal to twice the voice-coil length. Effectively, the reference structure is located at the extreme left of the graph where the two curves intersect.

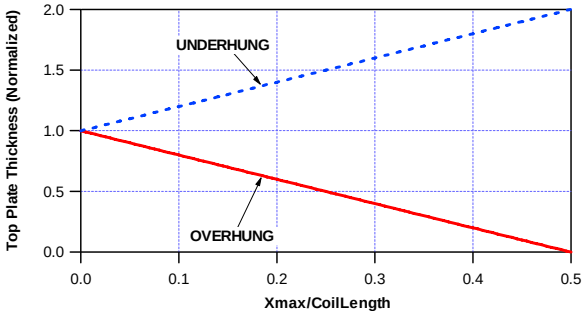

Fig. 5. Normalized underhung and overhung top-plate thickness as a function of the ratio between Xmax and the voice-coil length according to Eqs. 3 and 4.

2.3. Normalized Gap Flux Density

Expressions can be derived for the normalized gap flux density for the overhung and underhung structures. The derivation assumes no fringing.

The normalized flux density of the underhung structure is easy. It's constant and just equal to the flux density of the reference structure, i.e. the voice coil is always in the gap, no matter what its length, and must see the same flux density. This maintains the same Bl product no matter what the length of the underhung structure.

The normalized flux density of the overhung structure is not quite as simple. Because only a fraction of the voice coil is in the gap, the gap flux density must increase as the top-plate thickness is reduced in order to maintain a constant Bl product, i.e. the inverse of Eq. 3.

Therefore the normalized gap flux density for the overhung structure appears as:

$$B_{ONorm} = \frac{1}{1-2R} \qquad (5)$$

Note that the this flux density value rises towards infinity as R approaches 0.5 (the top plate thickness goes to zero), because of the inverse relationship.

Correspondingly, the normalized gap flux density for the underhung structure is constant and appears as:

$$B_{UNorm} = 1 \qquad (6)$$

Graphs of Eqs. 5 and 6 appear in the following figure. As before, effectively the reference structure is located at the extreme left of the graph.

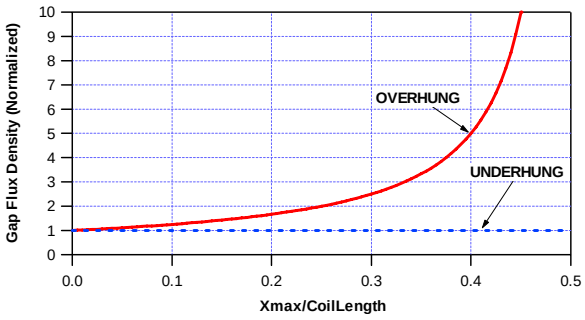

Fig. 6. Normalized underhung and overhung gap flux density as a function of the ratio between Xmax and the voice coil length according to Eqs. 5 and 6. Note that the overhung flux density rises very rapidly above 0.4 because the top plate thickness is getting quite small.

2.4. Normalized Gap Energy

The magnetic energy in a given volume of air depends on the magnetic field intensity H and the volume and is given by the following equation:

$$E = \frac{\mu_0}{2} H^2 V \qquad (7)$$

Where,

μ_0 = permeability of air

V = volume of air

In air, the flux density is given by $B = \mu_0 H$. With this knowledge, Eq. 7 can be converted to an expression in B and appears as:

$$E = \frac{1}{2\mu_0} B^2 V \qquad (8)$$

This of course agrees with the energy expression in Newman's memos.

The normalized gap energy for the underhung structure is straightforward because B is constant and the gap volume increases directly with the top-plate thickness. Thus through simple manipulation, the normalized underhung gap energy is given by:

$$E_{UNorm} = 1 + 2R \qquad (9)$$

The normalized gap energy for the overhung structure can also be calculated knowing that the gap flux density is given by Eq. 5 squared and the gap volume decreases directly with the top-plate thickness (Eq. 3) as follows:

$$E_{ONorm} \propto B^2 V = \left(\frac{1}{1-2R}\right)^2 (1-2R) = \frac{1}{1-2R} \qquad (10)$$

Fig. 7 shows plots of Eqs. 9 and 10. Note that the underhung gap energy only doubles over the plotted range, while the overhung gap energy rises rapidly for higher values of the ratio between Xmax and the voice coil length. As the top plate gets thinner, the gap energy rises very rapidly!

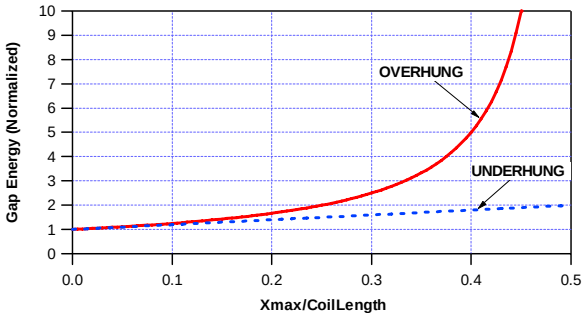

Fig. 7. Normalized underhung and overhung gap magnetic energy as a function of the ratio between Xmax and the voice coil length according to Eqs. 9 and 10.

2.5. Underhung-Overhung Energy Ratio

The gap energy ratio between the underhung and overhung motor structures is then given simply by:

$$\frac{E_u}{E_o} = \frac{E_{UNorm}}{E_{ONorm}} = \frac{1+2R}{\left(\frac{1}{1-2R}\right)} = (1+2R)(1-2R) = 1-4R^2 \qquad (11)$$

This of course agrees with Newman's expression of Eq. 1 and is plotted in Fig. 1.

With the added information leading to Eq. 11, we now know what Newman meant by the "no magnet required" case mentioned in the introduction. It's not that the underhung motor structure required no magnet, but that the overhung structure required an infinite amount of magnet! The ratio of the two energies falls to zero because the gap energy of the overhung motor is growing very large while the underhung gap energy stays finite (actually only doubles)!

3. SIMULATION

In this section, finite-element magnetic simulations were made of three loudspeaker motors:

1. a reference structure (top-plate thickness equal to voice-coil length),
2. an overhung structure, and
3. an underhung structure.

All three structures were designed to have similar shapes except for the changes required to switch from one shape format to the other. Newman's recommendations were followed: same excursion, same Bl product, and same voice coil. No special design techniques or optimization was used. Only gentle radiuses were applied to sharp corners. No thermal or cost issues were considered in the analysis.

Rather than use a permanent magnet, an electromagnet was used instead for simplification and ease of changing the magnet strength. The electromagnet skirted the problem of considering magnet materials, load lines and operating points. The electromagnet's magnetomotive force (MMF) could be directly set and tabulated in each design.

A voice coil of 300 turns was used to calculate the rest (mid) position Bl product. A large number of simulations were run under script control that varied the MMF of the electromagnet. At each value of MMF, various parameters were calculated including: Bl product, gap magnetic energy, core magnetic energy, fringe magnetic energy, and total energy. The middle two energies, core and fringe, are loss mechanisms. The total energy must be supplied by the magnet or the electro-magnet and is a direct measure of the amount of magnet required.

Three values of Bl product were chosen for simulation. Each simulation was accomplished for three different cases:

1. CASE 1: Perfect soft magnetic material and no fringing
2. CASE 2: Perfect soft magnetic material with fringing
3. CASE 3: Pure Iron soft magnetic material with fringing.

Details of these three cases follow in the next section.

3.1. Motor Structures

Three woofer motor structures were designed. Each had a 3"-diameter 1.5"-long voice coil of 300 turns. All the motors were designed to have a geometric *Xmax* of 0.6" (an *Xmax* to voice-coil length ratio *R* of 0.4). All were driven by an electromagnet, wound around the 2" diameter center pole, with a unit current drive and variable number of turns. The outside diameter of the structure was 5". Heights varied from 2.644" for the overhung structure, 3.25" for the reference structure, to 4.45" for the underhung structure.

Drawings of the three structures are shown in the next three sections.

3.1.1. Reference Motor (X_{max} = 0)

The reference motor is shown in Fig. 8 with a section through the center of the circular structure.

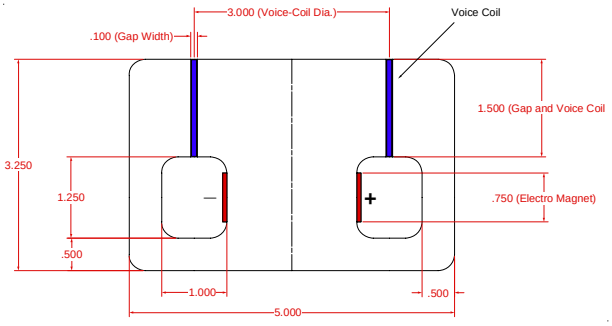

Fig. 8. Layout and dimensions of the reference motor structure. The top plate thickness is equal to the voice-coil length and both are 1.5". This results in a geometric X_{max} of zero. The electro-magnet is wound around the 2" diameter center pole.

3.1.2. Overhung Motor (X_{max} = 0.4L_{vc} = 0.6")

The overhung motor is shown in Fig. 9.

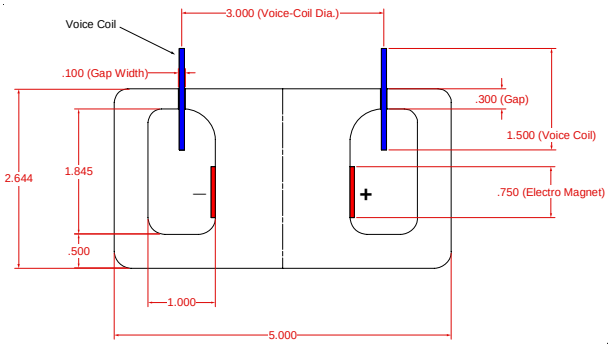

Fig. 9. Layout and dimensions of the overhung motor structure. The top plate is shorter than the voice coil. The top plate thickness is 0.3". The voice-coil length is 1.5". This results in a geometric X_{max} of 0.6".

3.1.3. Underhung Motor (X_{max} = 0.4L_{vc} = 0.6")

The underhung motor is shown in Fig. 10.

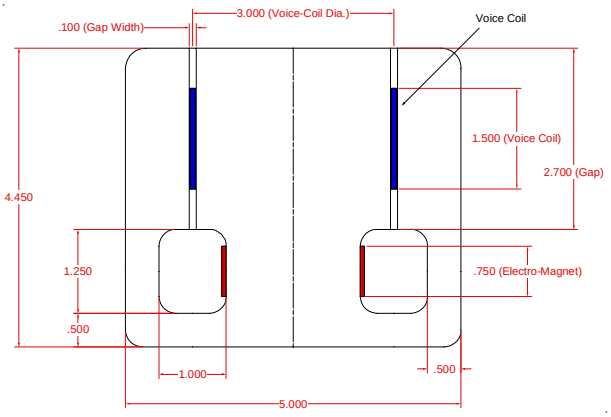

Fig. 10. Layout and dimensions of the underhung motor structure. The top plate is longer than the voice coil. The top plate thickness is 2.7". The voice-coil length is 1.5". This results in a geometric X_{max} of 0.6".

3.2. Simulation Setup

A commercially available finite-element magnetic simulator was used (FEMM: Finite Element Method Magnetics simulator version 4.0.1 available free from Foster-Miller Company:

http://www.foster-miller.com/magnetic_modeling.htm). The following subsections describe the boundary conditions and the setup for the three cases.

3.2.1. Boundary Conditions

An axisymmetric simulation region and boundary conditions are shown in the following figure. The circular boundary has a radius of 10" and uses FEMM's "mixed" Asymptotic Boundary Condition.

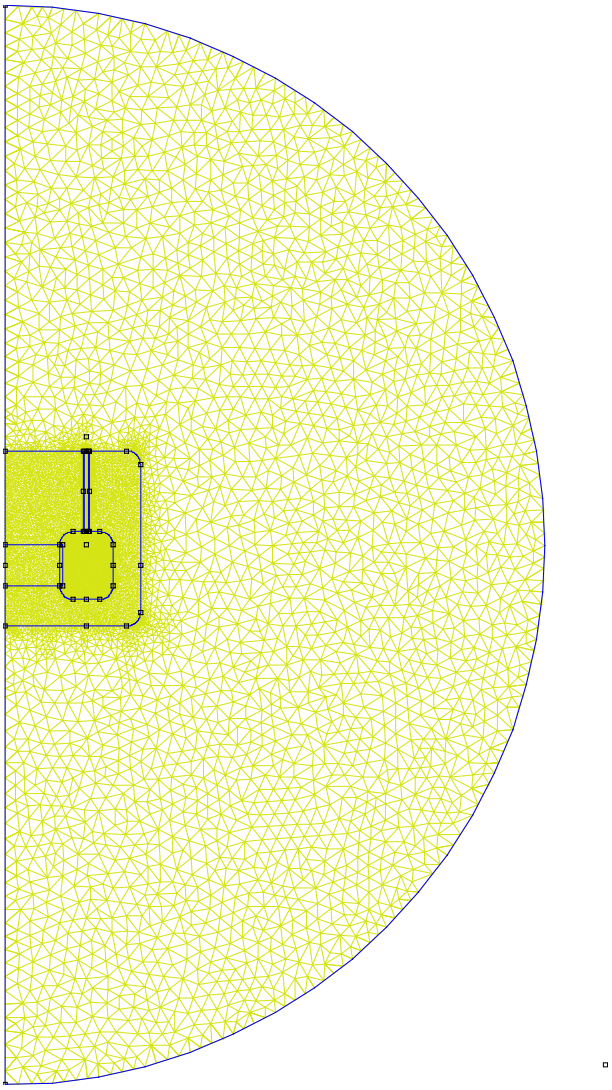

Fig. 11. Solution domain from FEMM simulator for the reference structure with finite element mesh. The axis of rotation is the vertical line on the left. The reference motor structure is shown.

The following figure shows the FEMM simulator setup for the reference structure setup for the CASE 3 condition.

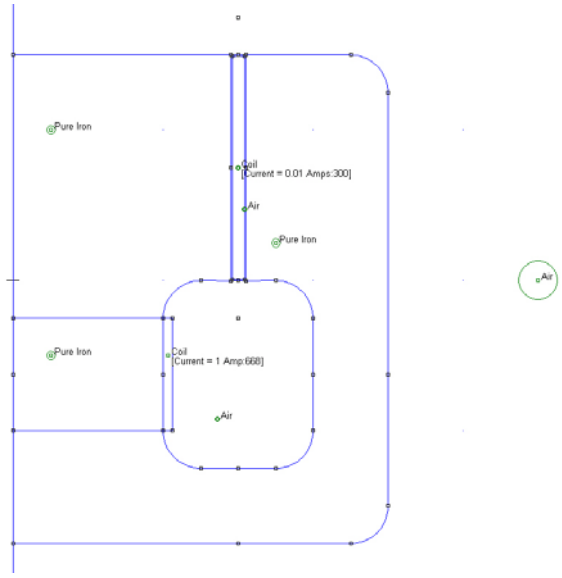

Fig. 12. Example FEMM solution setup for the reference motor assembly in the CASE 3 condition (Pure iron soft magnetic material with fringing).

3.2.2. CASE 1: Perfect Soft Magnetic Material and No Fringing

Conditions:

1. Linear soft magnetic material with a very high relative permeability (u_0 = 1 x 10^7).
2. Air with very low relative permeability of (u_0 = 1 x10^{-6}).
3. Gap air is normal with a relative permeability of unity (u_0 = 1).

This case corresponds to the conditions for Newman's energy derivation shown in Eq. 1 and Fig. 1.

3.2.3. CASE 2: Perfect Soft Magnetic Material with Fringing

Conditions:

1. Linear soft magnetic material with a very high relative permeability (u_0 = 1x10^7).
2. All air and air in gap is normal with a relative permeability of unity (u_0 = 1).

3.2.4. CASE 3: Pure Iron Soft Magnetic Material with Fringing

Conditions:

1. All air and air in gap is normal with a relative permeability of unity (u_0 = 1).
2. Use pure iron for all the metal parts with the B-H curve shown in the following figure.

Linear Horizontal H scale:

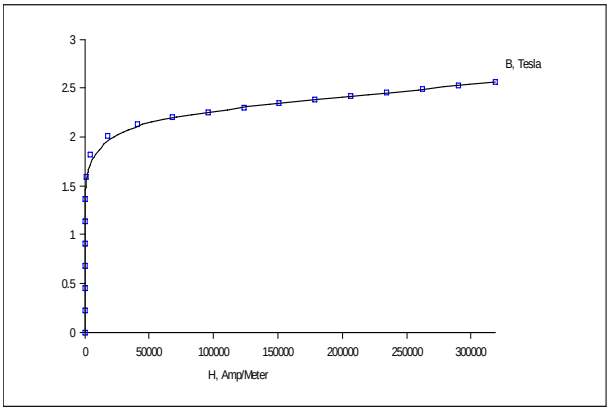

Logarithmic Horizontal H scale:

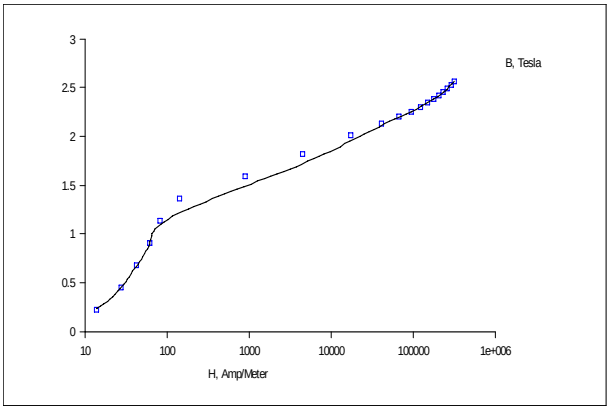

Fig. 13. B-H characteristics of pure iron as used in this paper's magnetic simulations. The plots were generated by the FEMM simulator. The solid line indicates the interpolated data that FEMM uses for its simulations. The vertical scale plots magnetic flux density B over the range of 0 to 3 Teslas. The horizontal scale plots the magnetic field intensity H in Amperes per meter. Linear horizontal axis (top graph), log horizontal axis (bottom graph).

3.3. Simulation Results

The following subsections illustrate the results of the FEMM simulations. The three motor structures (reference, overhung, and underhung) were analyzed in the three different CASE configurations described previously.

In every simulation, the exact same Bl product was maintained across the three different motor structures by individually varying the MMF of the electromagnet.

First a complete series of simulations were run to calculate magnetic energy in different parts of the motor and BL product as a function of the electromagnet's

MMF. After this, three different Bl products were chosen for detailed field simulations.

3.4. Compare Magnetic Field Energies

This section shows the results of a series of calculations varying the electromagnet's MMF to determine the motor structure's total magnetic field energy and resultant Bl product. The motor's total magnetic energy consists of three parts:

1. energy stored in the motor's voice-coil gap,
2. energy stored in the motor's soft metal core, and
3. energy stored in the fringe fields both inside and outside the core.

The sum of these three energies is the total magnetic energy. In an ideal motor, all the magnet's energy goes into the gap. Core and fringe energy are considered losses. The magnet must supply energy for all parts of the motor including the gap, core, and fringe. The total energy is then a good measure of the strength of the magnet required.

The two following subsections show the total energy and required magnet MMF as a function of Bl product for the three motor types.

3.4.1. Total Energy vs. Bl Product

The next figure shows how the motor's total magnetic field energy varies as a function of the driver's Bl product for the three motor types. The graph can be divided into two regions around a Bl of 18 T. Below this value, the underhung motor has less total energy than the overhung motor (as Ray Newman claimed). However, above this value, the situation is reversed. At a Bl of 18 T·m, the total energies are equal, which implies equal magnet requirements.

Above 18 T·m, the underhung structure's core energy (losses) starts increasing suddenly due to core saturation.

Based on these data, three Bl products of 10, 18, and 21.6 T·m were chosen for further detailed field analysis. These values were chosen to represent three distinct conditions where the underhung structure's total energy was significantly less, equal to, and more than the total energy of the overhung structure.

At each Bl value, detailed field simulations were run of the three motor types configured in the three CASE configurations. Also detailed numerical tables of motor parameters were generated at each Bl value and are displayed at the end of this paper.

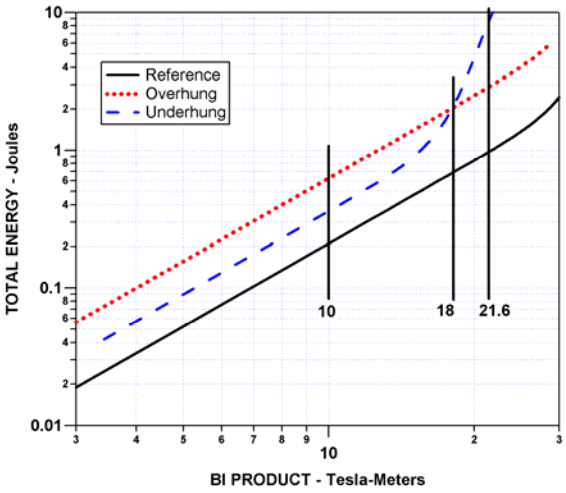

Fig. 14. Log-log plot of total magnetic energy versus Bl product for a voice coil of 300 turns in the CASE 3 reference motor structure (solid), overhung motor structure (dotted), and underhung motor structure (dashed). Note that total energy of the underhung and overhung motors crosses over at a Bl product of 18 T·m with the underhung motor having less energy than the overhung motor below this point, and greater energy above. The Bl product chosen for three magnetic simulations are indicated on the graph with vertical lines at Bls of 10, 18, and 21.6 T·m.

3.4.2. Magnetomotive Force (MMF) vs. Bl Product

The next figure shows the required value of the electromagnet's MMF that yields a specific Bl product. Note that the required MMF for the underhung structure starts rising rapidly above a Bl value of 10 T·m. Below the crossover point, the underhung motor requires significantly more MMF than the underhung motor.

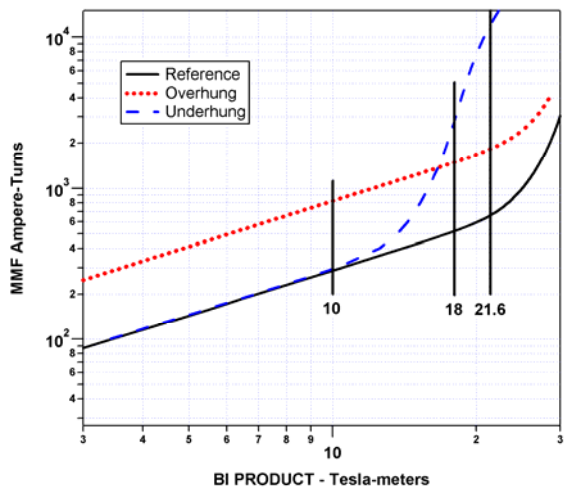

Fig. 15. Log-log plot of the required magnet magnetomotive force (MMF) versus Bl product for a voice coil of 300 turns in the CASE 3 reference motor structure (solid), overhung motor structure (dotted), and underhung motor structure (dashed). Note that the MMF for the underhung motor starts rising rapidly above a Bl of 10 T·m and crosses over the overhung structure at a Bl of about 16.6 T·m. As on the previous graph, the Bl product chosen for the three magnetic simulations are indicated on the graph.

3.5. Flux Density Field Plots and Gap Flux Density versus Position

This section shows the results of detailed field analysis run on the three motor types at the higher Bl value of 21.6 T·m where the underhung motor's total energy is higher than the overhung motor. All the flux density plots were run with a scale that that runs from 0 to 2.8 T (next figure). In addition to field plots, a graph showing the flux density along a line through the center of the gap is shown. Data is only shown for the CASE 1 and CASE 3 configurations to save space. Visually, the CASE 2 data appears similar to the CASE 3 data.

3.5.1. Flux Density Scale

The next figure shows the flux density grey scale for all the field plots. Flux density varies from 0 T (white) to 2.8 T (black). Values above 2.8 T are displayed as black.

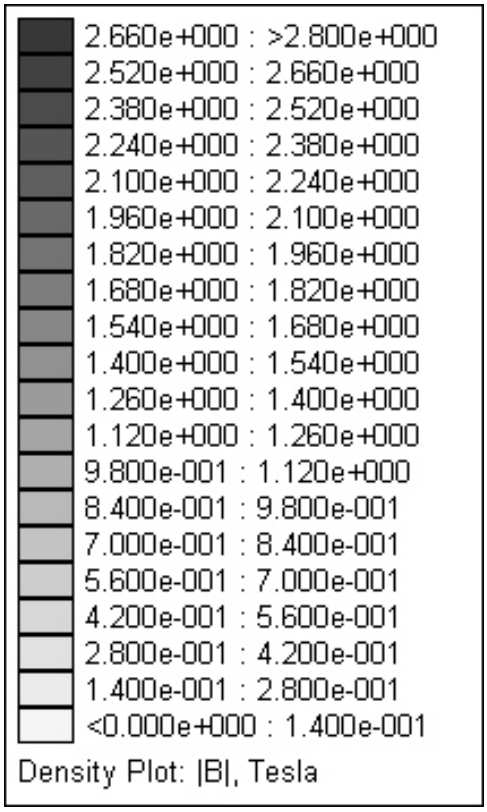

Fig. 16. Flux density shading scale ranging from 0 (bottom white) to 2.8 T (top black). Flux densities above 2.8 T appear as black.

3.5.2. CASE 1: Perfect Soft Magnetic Material and No Fringing

In CASE 1, the motor's metal parts are perfect with a linear B-H characteristic with a very high relative permeability of 10^7. This forces the H field in the metal to very-low values for reasonable B values. If H is very low the magnetic energy stored in the core is also very low.

Likewise fringing is minimized, by assigning a very low relative permeability of 10^{-6} to the air outside and inside the motor structure. The air in the gap remains at a relative permeability of unity, which is normal for air.

The next six figures show the flux density distribution and flux density along a line through the center of the gap for each of the three structures.

Reference Motor:

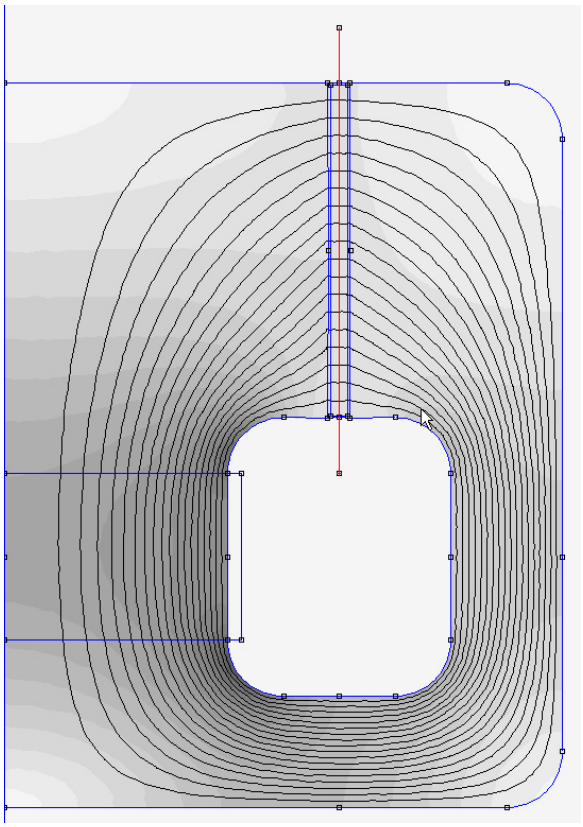

Fig. 17. CASE 1 flux density distribution for the reference motor structure for a Bl of 21.6 T·m. Refer to Fig. 16 for scale. Maximum core flux density of 2.2 T. The line in the center of the gap connecting two points outside the gap shows the path for the gap flux density versus position plots.

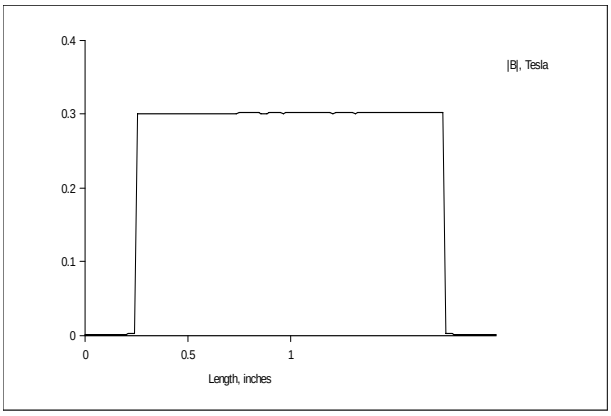

Fig. 18. Gap flux density vs. position along center of gap for the previous figure.

Overhung Motor:

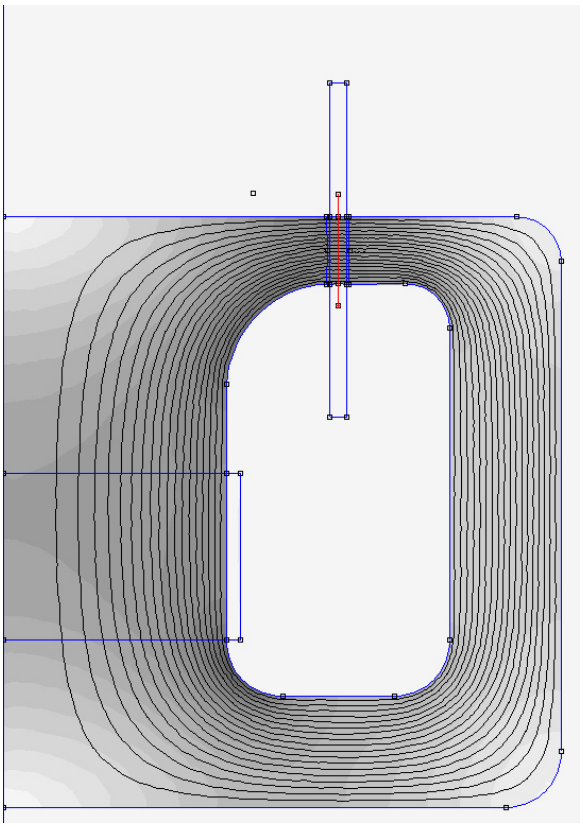

Fig. 19. CASE 1 flux density distribution for the overhung motor structure for a Bl of 21.6 T·m.. Refer to Fig. 16 for scale. Maximum core flux density of 2.2 T.

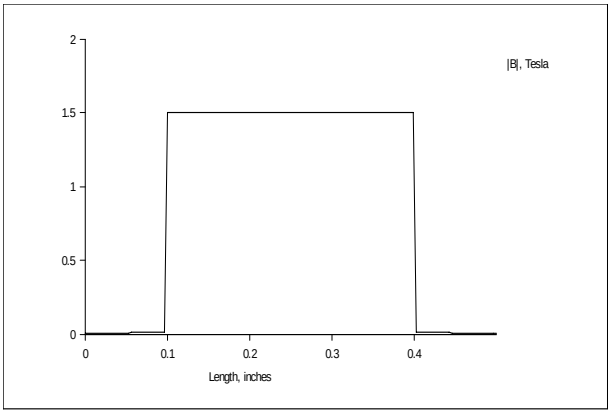

Fig. 20. Gap flux density vs. position along center of gap for the previous figure.

Underhung Motor:

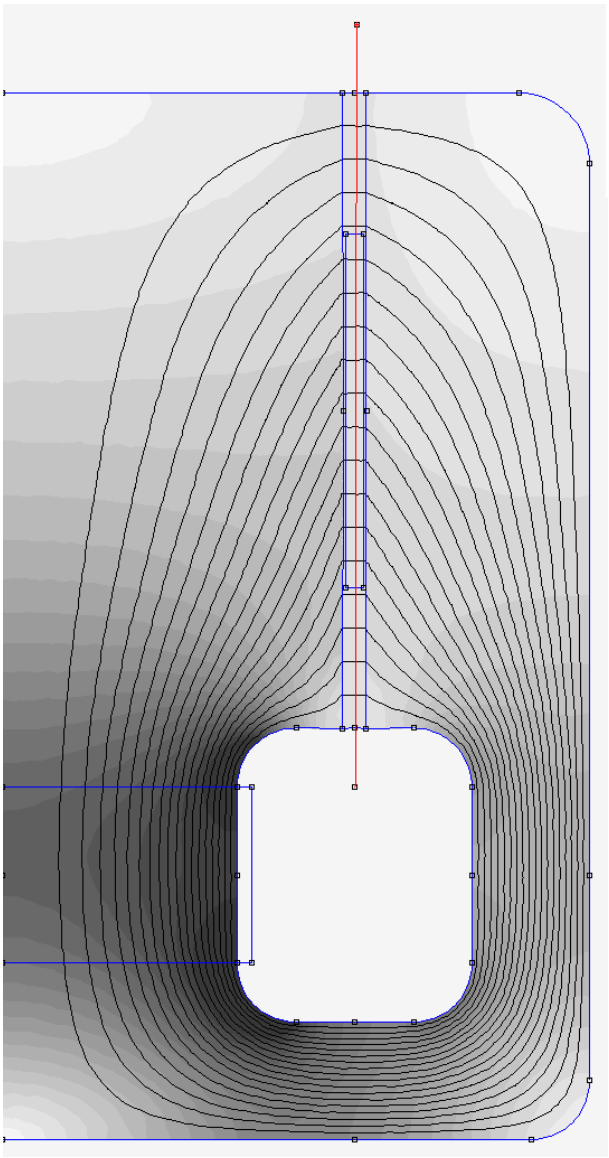

Fig. 21. CASE 1 flux density distribution for the underhung motor structure for a Bl of 21.6 T·m.. Refer to Fig. 16 for scale. Maximum core flux density of 3.9 T which occurs in the core adjacent to the electromagnet.

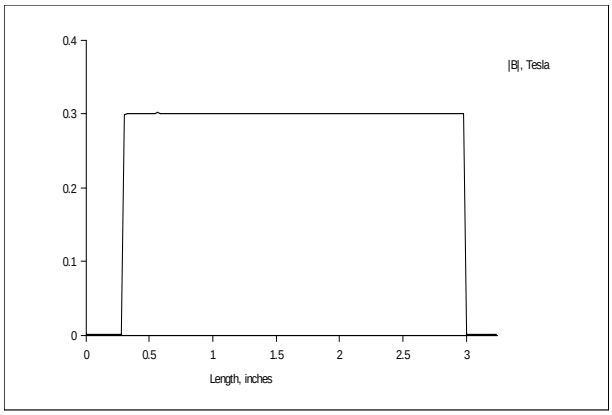

Fig. 22. Gap flux density vs. position along center of gap for the previous fugure.

Observations:

Note the absence of flux lines in all the field plots corresponding to no fringing. Note also the ideal rigid rectangular flat-top shape of the gap flux density along the center of the gaps.

3.5.3. CASE 3: Pure Iron Soft Magnetic Material with Fringing

In this case (CASE 3), the motor's metal parts are changed to pure iron. Pure iron is an ideal soft magnetic material for the metal parts because the iron has a relatively gradual B-H curve compared to other materials such as steel, i.e. it saturates gracefully. Unfortunately, because of rust problems, it is not commonly used. When the core is saturated, it sustains relatively high values of H for a specific B that implies high magnetic energy storage. This energy storage is a loss mechanism which needs to be minimized.

CASE 3 also allows normal fringing so that all the free space air has a unity relative permeability.

The next six figures show the flux density distribution and flux density along a line through the center of the gap for each of the three structures.

Reference Motor:

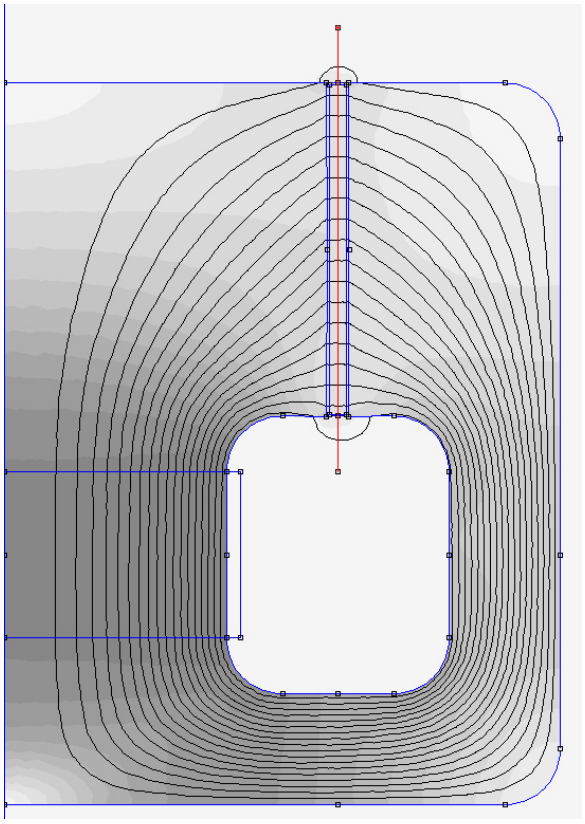

Fig. 23. CASE 3 flux density distribution for the reference motor structure for a Bl of 21.6 T·m. Refer to Fig. 16 for scale. Maximum core flux density of 1.6 T.

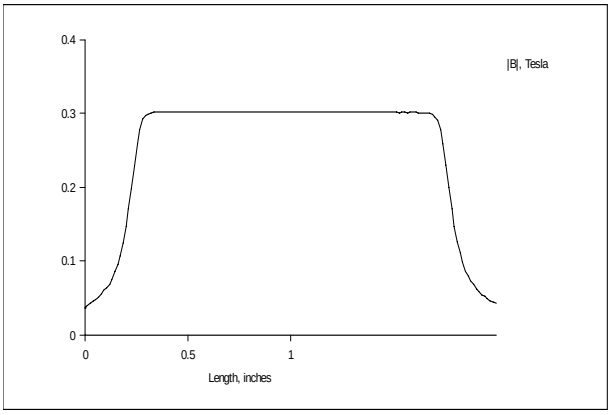

Fig. 24. Gap flux density vs. position along center of gap for the previous figure.

Overhung Motor:

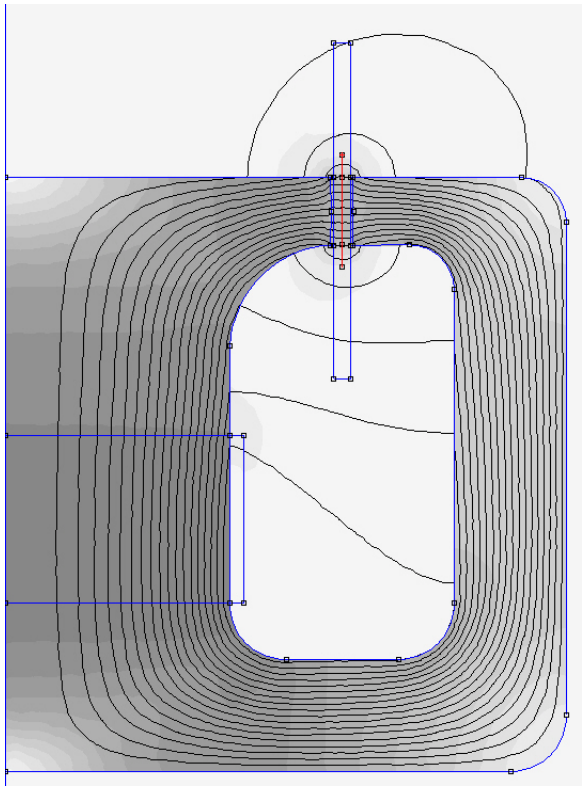

Fig. 25. CASE 3 flux density distribution for the overhung motor structure for a Bl of 21.6 T·m.. Refer to Fig. 16 for scale. Maximum core flux density of 1.7 T.

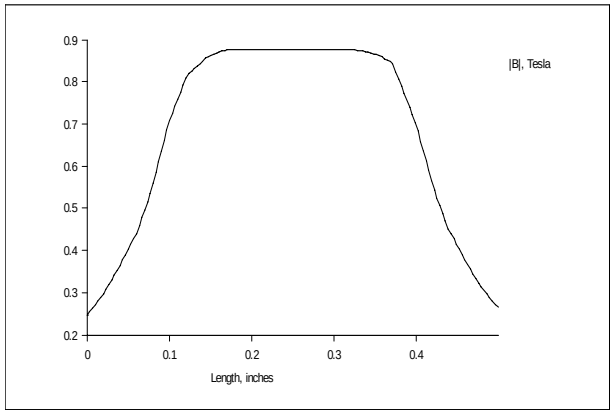

Fig. 26. Gap flux density vs. position along center of gap for the previous figure.

Underhung Motor:

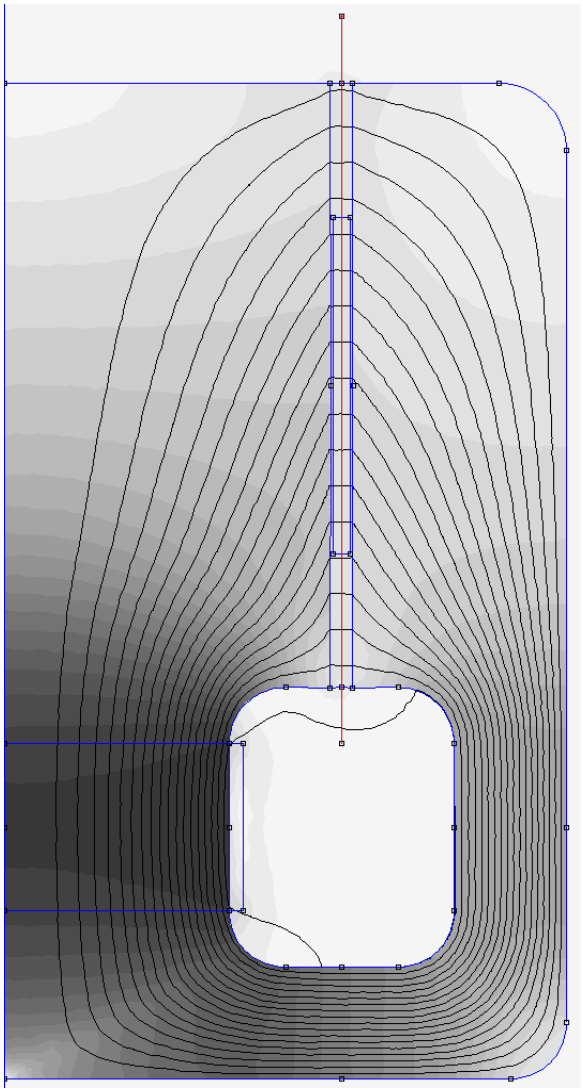

Fig. 27. CASE 3 flux density distribution for the underhung motor structure for a Bl of 21.6 T·m. Refer to Fig. 16 for scale. Maximum core flux density of 2.8 T.

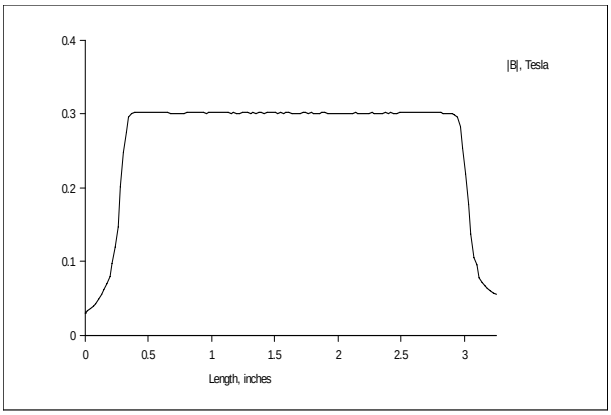

Fig. 28. Gap flux density vs. position along center of gap for the previous figure.

Observations:

Note the higher number of fringing flux lines both inside and outside the overhung structure as compared to the underhung and reference structures.

Note also that the gap flux density versus position graphs have a gentle flux-density roll off on either side of the flat-top region.

Also note that the maximum core flux density values (noted in the caption of each field plot) for the CASE 3 structures are significantly less than the CASE 1 structures.

3.5.4. Motor Structure Simulation Data Tables

A number of motor parameters were gathered for each analyzed situation including:

1. electromagnet MMF,
2. average flux density in gap (averaged along a line in the center of the gap from one edge of the gap to the other),
3. Bl product,
4. core flux,
5. gap reluctance,
6. core reluctance,
7. total reluctance,
8. gap magnetic energy,
9. core magnetic energy,
10. fringe magnetic energy, and
11. total magnetic energy.

These parameters are shown in tables 1, 2, and 3 (located at the end of the paper) for the respective Bl values of 10, 18, and 21.6 T·m.

Note that the tables show that when fringing is included (CASE 2 and CASE 3), the magnet requirements of the

overhung structure actually decrease as compared to the no fringe case shown for CASE 1 (compare the MMFs required in column two of each table for CASE 1 and CASE 2), because the fringe effectively lengthens the gap.

3.5.5. Comparison of Total Magnetic Energies for the Three Cases

This section shows bar graphs of the total magnetic field energy of the three structures (reference, overhung, and underhung) for each of the three cases described in Section 3.2. Three graphs are shown for the three different analyzed Bl-product values.

Bl = 10 T·m

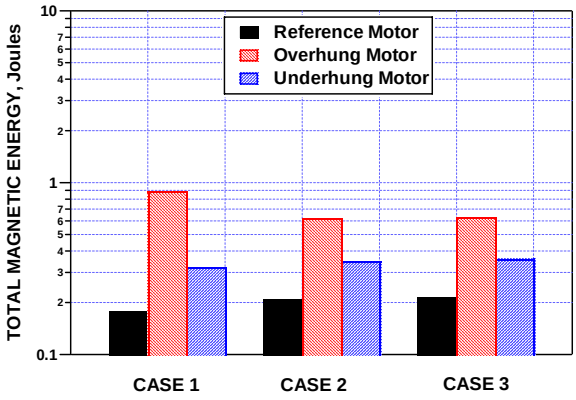

Fig. 29. Bar graph showing the total magnetic energy of the three structures for each of the three cases for a low-BL value of 10 T·m. Note that in every CASE the energy of the underhung motor is lower than the overhung motor.

Bl = 18 T·m

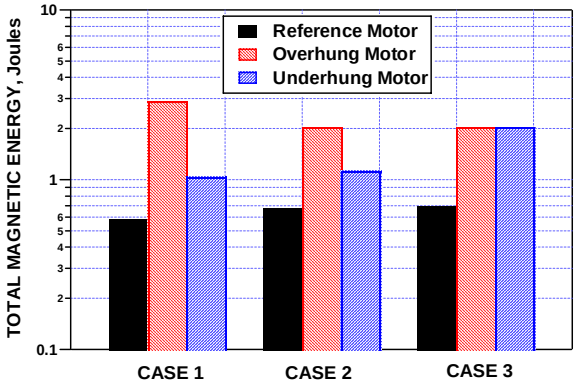

Fig. 30. Bar graph showing the total magnetic energy of the three structures for each of the three cases for a BL value of 18 T·m. Note that in CASE 1 and CASE 2 the energy of the underhung motor is lower than the overhung motor. However in CASE 3, the energies of the underhung and overhung motors are the same. This is not surprising because the BL value of 18 T·m was chosen to make them equal!

Bl = 21.6 T·m

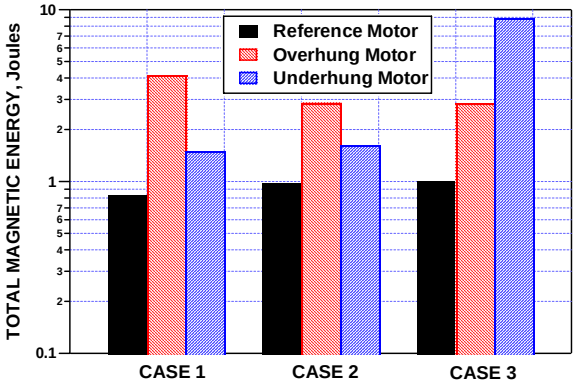

Fig. 31. Bar graph showing the total magnetic energy of the three structures for each of the three cases for a high-BL value of 21.6 T·m. Note that in CASE 1 and CASE 2 the energy of the underhung motor is lower than the overhung motor. However in CASE 3, the situation is reversed with the overhung lower than the underhung!

Observations:

These three bar graphs clearly show the dependence of the structure's total magnetic field energy on the Bl product, with the lower values providing underhung energies that are less than the overhung values.

3.5.6. Comparison of Fringe Magnetic Energies for the Three Cases

This section shows bar graphs giving the fringe magnetic field energy of the three structures (reference, overhung, and underhung) for the three cases described in Section 3.2. CASE 1 includes no fringing so its energy is zero. Three graphs are shown for the three different analyzed Bl-product values.

Bl = 10 T·m

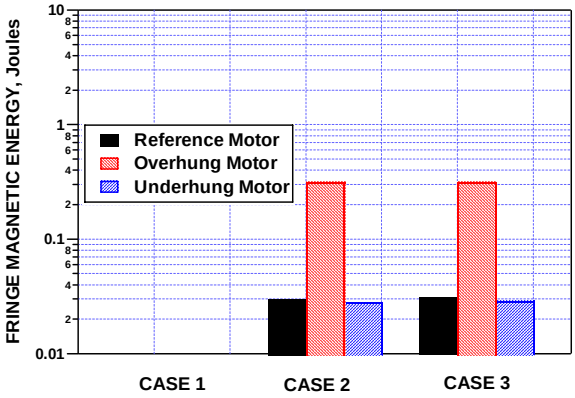

Fig. 32. Bar graph showing the fringe magnetic energy of the three structures for each of the three cases for a low-BL value of 10 T·m. Note that the fringe magnetic energy of the overhung motor is about 10 times higher than each of the other two motors.

Bl = 18 T·m

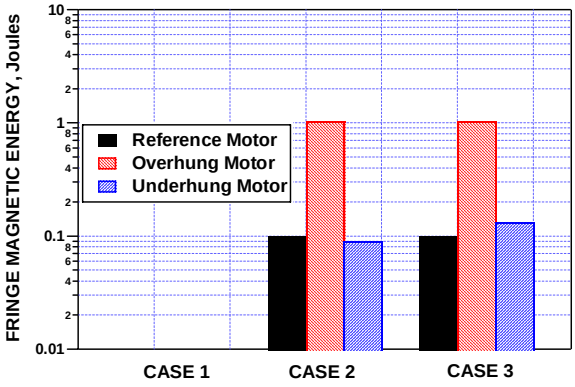

Fig. 33. Bar graph showing the fringe magnetic energy of the three structures for each of the three cases for a BL value of 18 T·m. As in the previous graph, the fringe magnetic energy of the overhung motor is about 10 times higher than each of the other two motors.

Bl = 21.6 T·m

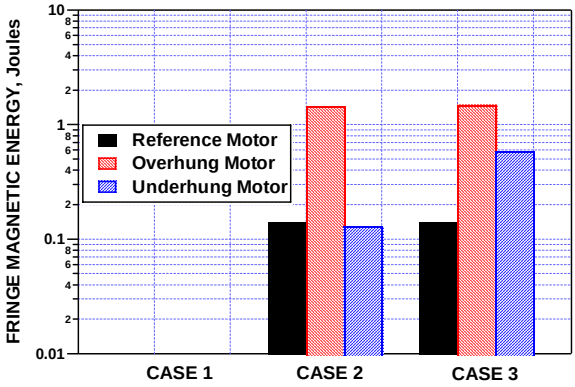

Fig. 34. Bar graph showing the fringe magnetic energy of the three structures for each of the three cases for a high-BL value of 21.6 T·m. Note that fringe magnetic energy of the overhung motor is greater than the other two structures. However, in CASE 3, the underhung energy has risen as a proportion of the overhung..

Observations:

These bar graphs clearly show that the fringing of the overhung structure is significantly higher than the reference and underhung structures.

4. CONCLUSIONS

This paper investigated the claims made by Ray Newman in his 1992 memo that the magnetic requirements of an underhung motor structure are less than an equivalent overhung structure. He assumed that the motors had the same excursion (X_{max}), the same efficiency (equal Bl products), have similar thermal behavior, and use the same voice coil. He also assumed that all the magnet's supplied energy ended up in the motor's voice-coil gap. This was the same as neglecting fringe and core magnetic losses.

This paper analyzed Newman's claims using newly derived equations and the latest finite-element magnetic simulation tools. The simulation analysis was based on three motor structures: 1. a reference motor structure with a geometric X_{max} of zero where the top-plate thickness was equal to the voice-coil length, 2. an overhung motor structure where the top-plate thickness is less than the voice-coil length, and 3. an underhung motor structure where the top-plate thickness is greater than the voice-coil length. Motor thermal issues were not considered in this paper.

All structures were of the "center slug magnet" style where the magnet is effectively completely enclosed by the metal structure. However, the analyzed structures all contained an electromagnet rather than a permanent magnet to simplify the motor simulations. The magnetomotive force of the electromagnet could be easily set and tabulated.

Each structure was analyzed under three conditions: 1. perfect soft magnetic material for the motor structure and no fringing, 2. perfect soft magnetic material for the motor structure with fringing, and 3. pure iron soft magnetic material for the motor structure with fringing.

With fringe and core magnetic losses included (the magnetic energy contained in the core and fringe fields), Newman's claim that an underhung motor structure requires less magnet than an equivalent overhung structure was verified only under a qualified condition. The condition was that the total flux of the underhung motor must be at or below an operating point where the core and fringe energy losses are approximately the same as the gap magnetic energy. For flux levels below this operating point, the underhung's magnet requirements are less than the overhung's requirements. If the flux is higher, then the underhung motor requires more magnet than the overhung motor because it's core losses are higher.

Of course the magnet is only one part of the cost of a motor assembly. In 1992, high-energy "neo" magnets were quite expensive as compared to ferrite magnets and Newman's claims of less magnet being required for an underhung structure were quite significant. Today, magnets are much cheaper and are a smaller percentage of the total driver cost.

The underhung motor structure requires over three times more magnetic flux than the overhung motor to maintain a given Bl product. This is due to its larger cross sectional gap area and the fringe field. The fringe field reduces the required core flux for the overhung motor but has no effect on the underhung motor. The increased flux is the main operational feature of the underhung motor structure that differentiates it from the overhung structure. This means that its core is significantly more prone to magnetic saturation than the overhung's structure assuming similar geometries. Another matter not covered in this paper is the amount of metal required for the core. The underhung structure requires slightly more that twice the core metal, by volume, than the overhung structure. This must be considered when making a choice between underhung and overhung motors.

Today, with the optimization capabilities of sophisticated finite-element magnetic driver-design simulators, the findings of this paper may be academic.

5. ACKNOWLEDGEMENTS

This work was supported by Harman International.

Many thanks go to Electro-Voice, division of Telex Communications and Bill Gelow (head of loudspeaker R&D) who gave permission to reveal and use the contents of Ray Newman's memos.

Much thanks also go to John Sheerin of Harman/Becker Automotive Systems who ran the magnetic simulations shown in this paper.

Thanks also to the co-authors of this paper who supported the idea of this paper and contributed technical comments and discussions on the topics covered in this paper.

Table 1: Motor Structure Simulation Data (Constant Bl Product, n = 300 turns, Bl = 10.0 T·m)

						Reluctance			Magnetic Energy		
Motor	**MMF**	**Average Flux Density in Gap , B**	**Bl Product**	**Core Flux**	**Gap**	**Core**	**Total**	**Gap**	**Core**	**Fringe**	**Total**
	Ampere-Turns	**Teslas**	**T·m**	**Webers x 10^{-3}**	**Rels x 10^{6}**	**Rels x 10^{6}**	**Rels x 10^{6}**	**Joules**	**Joules**	**Joules**	**Joules**
CASE 1:											
Reference	279	0.139	10.0123	1.27	0.220	0	0.220	0.178	0.28e-5	0	0.178
Overhung	1,401	0.697	10.0070	1.27	1.103	0	1.103	0.890	0.39e-5	0	0.890
Underhung	279	0.139	10.0137	2.29	0.122	0	0.122	0.321	0.97e-5	0	0.321
CASE 2:											
Reference	279	0.139	9.9996	1.27	0.220	0	0.220	0.179	0.38e-5	0.03	0.210
Overhung	816	0.396	10.0059	0.72	1.133	0	1.133	0.306	0.45e-5	0.316	0.622
Underhung	279	0.139	10.0137	2.28	0.122	0	0.122	0.321	1.13e-5	0.028	0.349
CASE 3:											
Reference	284	0.139	10.0298	1.27	0.2215	0.0021	0.2236	0.180	0.0030	0.031	0.214
Overhung	821	0.395	10.0041	0.72	1.1355	0.0048	1.1403	0.305	0.0035	0.317	0.626
Underhung	288	0.139	10.0012	2.28	0.1230	0.0033	0.1263	0.321	0.0096	0.029	0.360

Table 2: Motor Structure Simulation Data (Constant Bl Product, n = 300 turns, Bl = 18.0 T·m)

						Reluctance			Magnetic Energy		
Motor	**MMF**	**Average Flux Density in Gap , B**	**Bl Product**	**Core Flux**	**Gap**	**Core**	**Total**	**Gap**	**Core**	**Fringe**	**Total**
	Ampere-Turns	**Teslas**	**T·m**	**Webers x 10^{-3}**	**Rels x 10^{6}**	**Rels x 10^{6}**	**Rels x 10^{6}**	**Joules**	**Joules**	**Joules**	**Joules**
CASE 1:											
Reference	504	0.251	18.0432	2.29	0.220	0	0.220	0.579	0.93e-5	0	0.579
Overhung	2,528	1.256	18.0520	2.29	1.104	0	1.104	2.90	1.2e-5	0	2.90
Underhung	504	0.251	18.0462	4.125	0.122	0	0.122	1.04	3.2e-5	0	1.04
CASE 2:											
Reference	504	0.250	18.0210	2.28	0.221	0	0.221	0.580	1.2e-5	0.10	0.68
Overhung	1474	0.714	18.0577	1.30	1.134	0	1.134	0.997	1.5e-5	1.03	2.03
Underhung	504	0.250	18.0461	4.11	0.123	0	0.123	1.04	3.7e-5	0.09	1.13
CASE 3:											
Reference	522	0.252	18.1443	2.30	0.221	0.006	0.227	0.588	0.0114	0.10	0.70
Overhung	1,494	0.715	18.0802	1.30	1.137	0.012	1.149	0.999	0.0137	1.03	2.04
Underhung	2891	0.250	18.0354	4.10	0.123	0.582	0.705	1.043	0.8645	0.133	2.04

Table 3: Motor Structure Simulation Data (Constant Bl Product, n = 300 turns, Bl = 21.6 T·m)

						Reluctance			Magnetic Energy		
Motor	**MMF**	**Average Flux Density in Gap , B**	**Bl Product**	**Core Flux**	**Gap**	**Core**	**Total**	**Gap**	**Core**	**Fringe**	**Total**
	Ampere-Turns	**Teslas**	**T·m**	**Webers x 10^{-3}**	**Rels x 10^{6}**	**Rels x 10^{6}**	**Rels x 10^{6}**	**Joules**	**Joules**	**Joules**	**Joules**
CASE 1:											
Reference	604	0.301	21.6125	2.74	0.221	0	0.221	0.831	1.3e-5	0	0.831
Overhung	3,017	1.499	21.5433	2.74	1.101	0	1.101	4.13	1.8e-5	0	4.13
Underhung	604	0.301	21.6159	4.94	0.123	0	0.123	1.50	4.5e-5	0	1.50
CASE 2:											
Reference	604	0.300	21.5866	2.73	0.222	0	0.222	0.832	1.8e-5	0.14	0.972
Overhung	1762	0.854	21.6018	1.56	1.129	0	1.129	1.42	2.1e-5	1.45	2.87
Underhung	604	0.300	21.6159	4.92	0.123	0	0.123	1.50	5.3e-5	0.13	1.63
CASE 3:											
Reference	668	0.300	21.6068	2.73	0.222	0.024	0.245	0.834	0.0278	0.14	1.00
Overhung	1,849	0.854	21.6039	1.56	1.131	0.054	1.185	1.42	0.0357	1.48	2.86
Underhung	12,665	0.300	21.6021	4.92	0.123	2.451	2.574	1.50	6.85	0.59	8.94

6. PAPER REFERENCES

[1] A. N. Thiele, "Loudspeakers in Vented Boxes," J. Audio Eng. Soc., Part 1: vol. 19, no. 5, pp. 382-392, (May 1971), Part 2: vol. 19, no. 6, pp. 471-483, (Jun. 1971).

[2] R. H. Small, "Efficiency of Direct-Radiator Loudspeaker Systems," J. Audio Eng. Soc., vol. 19, no. 10, pp. 862-863 (Nov. 1971).

[3] R. H. Small, "Direct Radiator Loudspeaker System Analysis," J. Audio Eng. Soc., vol. 20, no. 5, pp. 383-395 (Jun. 1972).

[4] R. H. Small, "Closed-Box Loudspeaker Systems," J. Audio Eng. Soc., Part 1: Analysis, vol. 20, no. 10, pp. 798-808 (Dec. 1972), Part 2: Synthesis, vol. 21, no. 1, pp. 11-18 (Jan./Feb. 1973).

[5] R. H. Small, "Vented-Box Loudspeaker Systems," J. Audio Eng. Soc., Part 1: Small Signal Analysis, vol. 21, no. 5, pp. 363-372 (Jun. 1973), Part 2: Large Signal Analysis, vol. 21, no. 6, pp. 438-444 (Jul./Aug. 1973), Part 3: Synthesis, vol. 21, no. 7, pp. 549-554 (Sep. 1973), Part 4: Appendices, vol. 21, no. 8, pp. 635-639 (Oct. 1973).

[6] R. H. Small, "Passive-Radiator Loudspeaker Systems," J. Audio Eng. Soc., Part 1: Analysis, vol. 22, no. 8, pp. 592-601 (Oct. 1974), Part 2: Synthesis, vol. 22, no. 9, pp. 683-689 (Nov. 1974).

[7] R. J. Newman, "A High Quality All Horn Type Transducer," Presented at the 40th convention of the Audio Eng. Soc., preprint no. 784 (E-1) (Apr. 1971).

[8] R. J. Newman, "A Loudspeaker System Design Utilizing a Sixth-Order Butterworth Response Characteristic," J. Audio Eng. Soc., vol. 21, no. 6, pp. 450-456 (Jul./Aug. 1973).

[9] R. J. Newman, "Particular vented-Box Loudspeaker System Based on a Sixth-Order Butterworth Response Function," J. Acous. Soc. Am., vol. 55, Issue S1, pp. S29-S30 (Apr. 1974).

[10] R. J. Newman, "On the Measurement and Interpretation of a Modified Form of Qts as a Means of Controlling the Loudspeaker Quality," Presented at the 40th convention of the Audio Eng. Soc., preprint no. 960 (N-2) (May 1974).

[11] D. B. Keele, Jr. and R. J. Newman, "Application of Recent Australian Loudspeaker Research to Producible Loudspeaker Systems," Presented at the

IEEE International Conference on Acoustics, Speech, and Signal Processing (ICASSP'76), (Apr. 1976).

[12] R. J. Newman, "Dipole Radiator Systems," J. Audio Eng. Soc., vol. 28, no. 1/2, pp. 35-39 (Jan./Feb. 1980).

[13] R. J. Newman, "High Output Loudspeaker for Low Frequency Reproduction," United States Patent No. 4,733,749 (Mar. 1988).

[14] R. J. Newman, "Do You Have a Sufficient Quantity of Acoustical Benzin?-Aspects Related to the Significance of Diaphragm Excursion," Presented at the 80th convention of the Audio Eng. Soc., preprint no. 2342 (K-5) (Mar. 1986).

[15] R. J. Newman, "New Magnetic System Designs for Sound-Reinforcement Loudspeaker Applications," J. Audio Eng. Soc., vol. 37, no. 4, pp. 215-225 (Apr. 1989).

[16] Ray J. Newman, "A. N. Thiele, Sage of Vented Boxes," *Audio Magazine* (Aug. 1975).

[17] Ray Newman, "A Systematic Approach to Loudspeaker Design, " *Stereo Review Magazine*. (Aug. 1981).

[18] S. Mowry, "An Interview with Neville Thiele," *Voice Coil Magazine*, (Jan. 2006).

7. APPENDIX 1: NEWMAN'S THREE MEMOS

The following sections show copies of Ray Newman's Electro-Voice memos of 1992 (with the permission and courtesy of Electro-Voice, Division of Telex Communications).

7.1. Memo 1: "An Important Aspect of Underhung Voicecoils", May 8, 1992

FAX 616/695-1304

Electro-Voice®
a MARK IV company

PHONE 616/695-6831

BUCHANAN, MICHIGAN 49107

INTER-OFFICE CORRESPONDENCE

To: Distribution

Date: May 8, 1992

From: Ray Newman

Subject: An Important Aspect of ~~Underhung Voicecoils~~

CONFIDENTIAL

cc: Al Watson, Paul Fidlin, Matt Ruhlen, Kent Frye, David Calrson

A most interesting problem involves considering a set of related underhung and overhung magnetic assemblies that are so constructed so as to have:

a. the same Xmax
b. the same efficiency
c. similar thermal behavior
d. the same voicecoil.

By considering these coils operating in a gap whose gap energy is

$W=BV/2u$ (B=flux density, V=gap volume and u is the permeability of air)

it is possible to express the ratio Wu(underhung)/Wo(overhung) as a function of Xmax and K, the coil length. Without going through the steps to get there (this is left as an exercise for the student), the result is:

$Wu/Wo=1 - 4(Xmax/K)**2. = 1 - 4\left(\frac{Xmax}{K}\right)^2$

This somewhat remarkable result is plotted on the attached figure with the typical woofer range of Xmax/K noted.

When it is realized that the ratio Wu/Wo is also the ratio of respective magnet masses, the figure indicates reductions of .9 to .4 in this important component. Think Neodymium.

I will be glad to explain the "no magnet needed" case (Wu/Wo=0) to anyone who is curious.

Ray Newman

Ray Newman

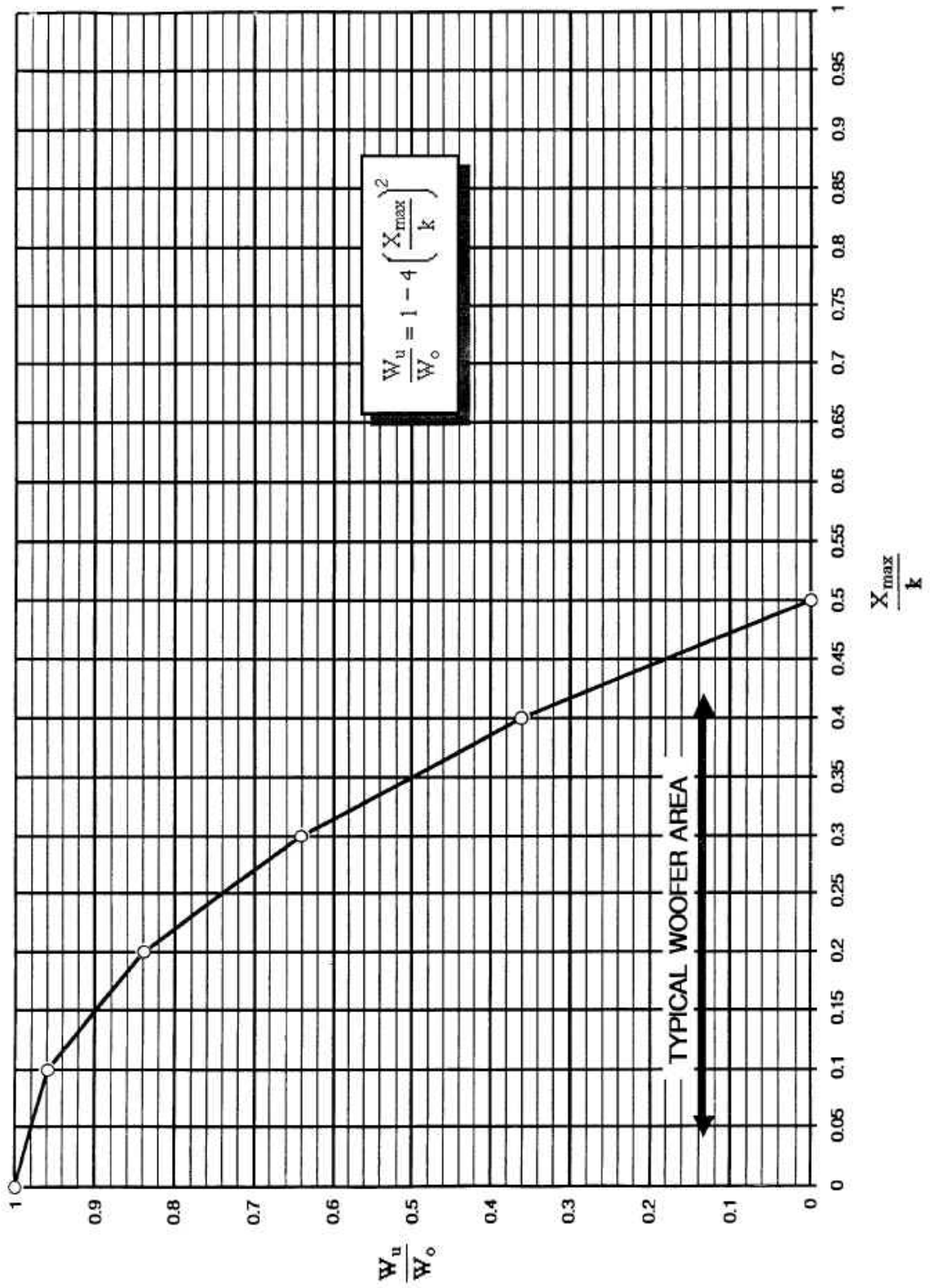
$\frac{W_u}{W_o} = 1 - 4\left(\frac{X_{max}}{k}\right)^2$
TYPICAL WOOFER AREA
$\frac{W_u}{W_o}$
$\frac{X_{max}}{k}$
1
0.9
0.8
0.7
0.6
0.5
0.4
0.3
0.2
0.1
0
0.05
0.15
0.25
0.35
0.45
0.55
0.65
0.75
0.85
0.95

7.2. Memo 2: "Underhung 2", May 18, 1992

FAX: 616/695-1304

Electro-Voice®
a MARK IV company

PHONE: 616/695-6831

BUCHANAN, MICHIGAN 49107

CONFIDENTIAL

INTER-OFFICE CORRESPONDENCE

To: Distribution

Date: May 18, 1992

From: Ray Newman

Subject: Underhung 2

cc: Al Watson, Paul Fidlin, Matt Ruhlen, Kent Frye, David Carlson

Two additional matters:

1. Attached is a derivation of the total useful flux passing through an underhung magnetic system based on "duplicating" the performance of a overhung system. I've taken the liberty of xeroxing a page from my notebook to illustrate the situation. Note that this implies something about the mass of steel needed by the structure to support flux. The geometry proposed by Kent Frye involving using small volume, high energy magnets as a pole face is attractive on this account. It should tend to minimize steel under high flux conditions.

2. Also attached is another version of the W_g/W^5 graph. The "typical woofer area" really should go from about 0.25 (DLX) to perhaps 0.4 (W-series and beyond).

Ray Newman

Ray Newman

MR

Page No. 5-11-92 (Mon)

A second derivation involves the amount of flux going thru the centerpole and base of the top plate.

Going from $\frac{W_U}{W_0} = 1 - 4\left(\frac{X_m}{K}\right)^2$, we must solve for B_U/B_0 & multiply by gap lengths (L) for Φ_U/Φ_0. (Recall $L_0 = K - 2X_{MAX}$ & $L_U = K + 2X_{MAX}$)

Since Gap energy $\propto B^2V$

$$\frac{B_U^2 V_U}{B_0^2 V_0} = 1 - 4\left(\frac{X_m}{K}\right)^2$$

$$\frac{B_U^2}{B_0^2} = \frac{V_0}{V_U}\left[1 - 4\left(\frac{X_m}{K}\right)^2\right]$$

$$\frac{B_U}{B_0} = \left(\frac{V_0}{V_U}\right)^{1/2}\left[1 - 4\left(\frac{X_m}{K}\right)^2\right]^{1/2}$$

gap lengths; gap vol (thickness drops out in ratio)

$$\frac{B_U L_U}{B_0 L_0} = \frac{\Phi_U}{\Phi_0} = \frac{K+2X_m}{K-2X_m}\left(\frac{K-2X_m}{K+2X_m}\right)^{1/2}\left[1 - 4\left(\frac{X_m}{K}\right)^2\right]^{1/2}$$

$$\boxed{\frac{\Phi_U}{\Phi_0} = \left(\frac{K+2X_m}{K-2X_m}\left[1 - 4\left(\frac{X_m}{K}\right)^2\right]\right)^{1/2}}$$

(i.e. take old $\frac{W_U}{W_0}$, mult by ratio of gap lengths and take $\sqrt{\ }$)

Ex. 1 (from Pg 150); $W_U/W_0 = .5$, $X_m = .5$, $K = 1.4$

$$\frac{\Phi_U}{\Phi_0} = \left(\frac{2.4}{.4}[.5]\right)^{1/2} = 1.73$$

Ex 2 (Simi. to W woofers); $W_U/W_0 = .7$, $X_m = .25$, $K = .9$
$\Phi_U/\Phi_0 = 1.56$

Then suggest 3-3½" centerpoles/magnets ... To Page No. ___

Witnessed & Understood by me,	Date	Invented by	Date
		R Newman	5-11-92
		Recorded by	

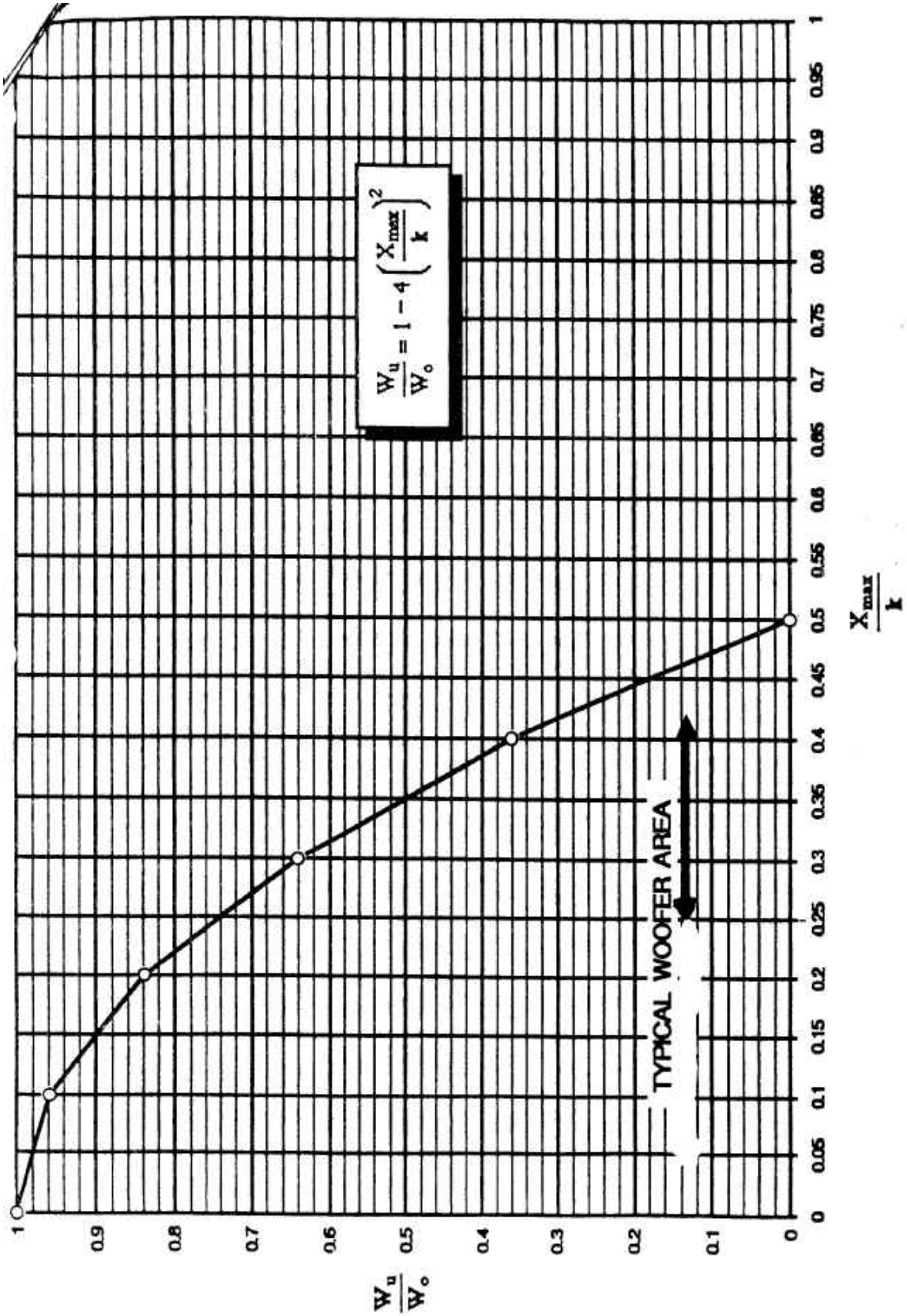
$\frac{W_u}{W_o} = 1 - 4\left(\frac{X_{max}}{k}\right)^2$
TYPICAL WOOFER AREA
$\frac{W_u}{W_o}$
$\frac{X_{max}}{k}$
1
0.9
0.8
0.7
0.6
0.5
0.4
0.3
0.2
0.1
0
0.95
0.9
0.85
0.8
0.75
0.7
0.65
0.6
0.55
0.5
0.45
0.4
0.35
0.3
0.25
0.2
0.15
0.1
0.05
0

7.3. Memo 3: "Underhung 3", Dec. 11, 1992

FAX: 616/695-1304

Electro-Voice®
a MARK IV company

PHONE 616/695-6831

BUCHANAN, MICHIGAN 49107

INTER-OFFICE CORRESPONDENCE

To: Distribution Date: December 11, 1992

From: R. Newman Subject: Underhung 3

CONFIDENTIAL

Dist: A. Watson, P. Fidlin, K. Frye, K. Walker, D. Carlson, D. Gunness, M. Ruhlen

ABSTRACT. An expression is derived and presented which shows the effect, on the amount of magnetic material, resulting from switching to an underhung (UH) coil geometry. Examples are presented which indicate very favorable reductions in magnet size for the case of long excursion woofers. In extreme cases, the reduction might be sufficient enough to convert a overhung (OH) ferrite loudspeaker into an underhung (UH) neodymium version at little cost penalty. The text emphasizes two additional matters. The first being that typically most (but not all) of the potential magnet size reduction is due to the OH to UH conversion rather than any switch from ferrite to a high energy material such as neodymium. The second has to do with the increased center pole flux that UH geometries must carry and the problems that may result.

It is evident from this study that the underhung geometry has not been examined in detail. If it had been, there would be many more loudspeakers out there that would be of this type.

BACKGROUND. Back in early '92 I was working with underhung coil geometries (see "Underhung 1 and 2" memos of May 8 and May 18) and derived a relatively simple equation that indicated a potential decrease in magnet size when an overhung motor geometry was switched to a similar performing underhung geometry. The decrease alluded to was in the range of .9 to .4, depending upon the specific geometry. This equation was based upon an Xmax equal to the geometric Xmax (which I call Xgm). (This is the excursion at which the coil begins to leave the physical gap which is set by the space defined inside the i.d. of the top plate of the magnetic structure.) These studies do not form a complete picture as the coil can go some additional distance before distortion becomes gross. Reality notwithstanding, this simplified picture indicated an appreciable magnet volume reduction for large excursion woofers. This reduction is primarily due to a long coil which, in the underhung (UH) case, is completely immersed in the gap flux.

A THREE TERM EXPRESSION FOR MAGNET SIZE CHANGE. I wish to expand this study by accounting for some "coil overrun" and the more compacted geometry caused by smaller magnets. Bringing in these two additional factors results in a three term expression shown in appendix X.

Page 2

The expression is in the form:

Magnet Change = A x B x C
Here A is the previously derived expression (see "Underhung 1")
B is a modifier allowing for voice coil overrun
C is a factor accounting for leakage change due to magnet geometry changes.

Note that a switch from overhung (OH) to underhung (UH) can change all three terms in the equation. (Usually the first two terms are the most affected.) A change that involves a higher energy magnetic material, however, will only change C, the leakage factor term.

A few additional comments are in order for the three termed expression and then a few examples will be shown to illustrate what is going on.

The A term, as noted earlier, accounts for the change in magnetic material volume resulting from switching to an UH geometry with Xmax equal to Xgm. It was derived by considering the change in gap energy $W=KB^2V$ (where K is a constant, B is flux density and V is gap volume).

The B* term factors in the effect of a chosen degree of voice coil overrun which is indicated by the fraction "f". (If one-eighth of the coil is permitted to exit the physical gap, then f equals one-eighth.) David Gunness uses $1-f^{.7}$ or about one-sixth in his design work as this amount correlates reasonably well with the onset of appreciable (10%) total harmonic distortion. This factor favors UH geometries because they have less abrupt skirts on their BL profile resulting in more "soft clipping" which is beneficial. It is not unusual to have term B comparable to term A in value.

Term C, a leakage factor term, accounts for a change in magnetic leakage flux that yields an increase in gap flux. This suggests a further reduction in magnet size to compensate for the increase. The leakage flux can be comparable to or exceed the usable flux in the gap. Moderate changes in magnetic system diameter might net

---

* Strictly speaking, this factor assumes that the overrun will be taken advantage of by adjusting (lengthening) the coil. This results in a corrective decrease in the gap flux density B. The other way of taking advantage would be through maintaining coil length and reducing the gap height and hence, gap volume. The two methods should yield similar magnet size reductions.

Page 3

something of the order of .8 or .9 for this term. More radical changes, including new magnet geometries (such as making the magnet into a pole face) might give values like .6 to .4. The meaning of this term (and the whole equation as well) can be confusing when a change in magnetic material is involved. High energy materials (like N/D) are about the only way C values less than .7 can be achieved. When this happens, the magnet change equation indicates a reduced amount of original magnet material (typically ferrite) whose gap energy needs to be matched with an appropriate amount of the new material. This is because the equation was derived based on required gap energies and is "blind" to the type of magnet used.

As a matter of interest, the C resulting from a ferrite geometry converted to the most efficient alnico geometry known is about .6. Going from a ferrite structure to one so efficient it has no leakage flux would net approximately .2. Half way between would be .4. My inclination is to use .6 in examples to follow that have a switch in magnet material.

Neodymium has roughly 10 times the energy product and 1.5 the density of ferrite which suggests a net weight reduction of .15. As an example, if a ferrite magnet of 100 oz. is downsized to 25 oz. by converting to UH (and you've cleverly already used a C value of, say, .6 because you knew you wanted to use a high energy material), the final weight would be 25x.15 or about 4 oz. A prime mark (') will be used to differentiate a switch-of-material computation from a nonswitched one. The meaning of a primed quantity should be taken as a "magnet equivalent" factor--i.e. the amount of new (usually N/D) material required to give the same gap energy as the computed fractional amount of the original (usually ferrite) material. The "magnet equivalent" quantity is tied to a C value below about .7 which implies high energy magnet materials used efficiently.

Note that to get enough change in magnet size to afford an N/D switch, means the AxB part of the equation must already be small (approximately below .5). This, coupled with a healthy C reduction, may drive the magnet down to one-forth the original size or lower. In other words, the way needs to be cleared by a favorable AxB reduction before changing to a high energy magnet material like N/D.

The possible result of all this (besides getting UH configurations and the dazzle of neodymium) is to get lighter weight high excursion woofers at costs approaching the current norm. Cutting weight by a factor of .7 to .5 might be possible. In addition, the increased coil surface area, well buried in the gap, should have some thermal advantage.

Page 4

EXAMPLES. Three examples are given in appendix Y. The first example has a overhung situation not unlike a DL18W. The second example is a more ambitious woofer, similar to an EVX-1500, with a very long coil. Both cases are computed for a permitted overrun of one-sixth of the coil length. The leakage factors chosen range from a moderate .8 to a substantial .6. Note that these two woofers have X(one-sixth) values of .27 inch and .57 inch which represent moderate and quite large excursion values that are separated by a factor of two. As a contrast, a third example is included; that of a low excursion woofer similar to a DLX. Here X(one-sixth) would be .17 inch and the chosen leakage factor is .9.

The reductions in magnet size in these three examples range from .22 (the highest excursion woofer having a C value associated with a N/D switch) to .7 (the low excursion woofer with a C value associated with keeping ferrite).

COSTS. The effect of these magnet changes on total woofer cost is both a matter of special interest and one that can be misleading if one is not careful.

In most medium to high production ferrite magnet loudspeakers, the cost of the magnet is typically a small part of the total VMC (usually around 10%). Therefore, reducing magnet size substantially can only influence total cost in a minor way. This suggests, however, that a OH to UH conversion can be accomplished without penalty.

In the case of a OH neodymium loudspeaker, the cost of the magnet can be twice that of the VMC of the rest of the unit. Here a substantial reduction in magnet can mean a great deal. A one-forth size magnet can mean a reduction in magnet cost from $80 to $20. In the case of a $50 VMC ferrite OH loudspeaker, whose N/D counterpart could cost $125, the reduced cost from going to a UH unit might result in a total VMC of $65. This would amount to a cost that would be 1.3 that of the original ferrite unit---a very attractive result. A one-eighth size magnet would cause the total VMC to become $55, a cost of 1.1 that of the original ferrite unit---virtually the same cost. Observe that in making these rough cost comparisons, the cost of the magnetic circuit steel parts has been left unchanged. This was done in an attempt to account for the longer UH gap by assuming this gap would offset savings from smaller diameter plates.

Let me recap. A magnet size reduction due to converting an OH to an UH magnetic geometry has a small effect on VMC when magnet cost is

a small part of the total VMC (as ferrite magnets typically are). However, when magnet cost dominates the loudspeakers VMC (typical of OH N/D units), the reduction in total VMC from a switch to an UH geometry can be dramatic. If the reduction is large enough, it is possible to approach the cost of a comparable ferrite magnet loudspeaker.

MAGNETIC FLUX CONSIDERATIONS. The large area magnetic gap in a UH loudspeaker requires a larger amount of magnetic flux in the magnetic systems steel parts.In particular, the center pole (which could be running close to magnetic saturation in the OH case) is affected. An expression is derived for flux change when going from an OH to UH geometry and is presented in appendix Z. The three examples shown in appendix Y would have flux increases of 1.34, 1.47 and 1.22 respectively. These are proportional to the loudspeakers Xmax values of .27, .57 and .17 respectively. In the case of a 2.5-inch centerpole loudspeaker running close to magnetic saturation, the conversion from OH to UH may require a larger center pole (and voice coil) to carry the increased flux. It is conceivable, that in some cases where the gap diameter is already large, that the UH version may be very difficult to make. In any case this matter needs to be considered.

OTHER CONSIDERATIONS. The X(one-sixth) value typically used in this memo is experimentally derived. It is the result of two factors that are interacting; gap fringing flux and coil overrun past the effective fringing flux region. It is expected that a more detailed study of this matter will not markedly change the results presented here, but the situation needs further investigation.

As mentioned above, it may sometimes be necessary to increase gap diameter to handle increased flux levels in metal parts. The effect of this maneuver needs to be understood.

SUMMARY. The relationships that have been derived and presented here are of a fundamental nature and deal with subject material that seems to have received little prior attention. The results are that underhung (UH) magnetic configurations, when compared to the much more common overhung (OH) type, have some favorable performance characteristics which are not readily obvious. In fact, "common sense" (larger gap means larger magnet) would lead you in the wrong direction. This presentation is not an all inclusive one in that there are several areas mentioned such as fringing flux effects and the ramifications of increased centerpole flux which should be explored further. What has been presented suggests the following comments which have been ordered by the degree of "woof" your woofer possesses. (See text for examples.)

Page 6

1. On low excursion loudspeakers (Xmax below .2 inch) an OH to UH conversion can be made with little or no cost penalty. (The magnet might be somewhat smaller, but probably not enough to offset the metal parts needed to construct the extended UH gap.) Switching to neodymium here would be quite expensive, perhaps nearly doubling the cost. A special case in this category is that of a loudspeaker which has the coil being the same length as the gap (such as an EVM). Here Xgm is zero. This causes terms A, B and C of the three term expression to all go to one assuming magnet type is not altered. This agrees with reason as here OH and UH have no meaning--i.e. they're both the same thing.

2. On high excursion loudspeakers (Xmax between about .2 and .4 inches) the magnet size reduction becomes more substantial and reaches values of one-half or so. Such reductions are not enough to suppress the total cost of the woofer appreciably. A switch to neodymium in this class unit will result in a substantial cost increase. Roughly speaking, we might be talking 1.5 times as much total cost rather than about twice as much for the case of keeping the loudspeaker as an OH unit.

3. On very high excursion loudspeakers (Xmax above .4 inch) the reduction in magnet can become dramatic and may be enough to permit a switch to neodymium at a relatively small cost penalty when compared to the corresponding ferrite magnet OH format loudspeaker. Here, however, high centerpole flux (see appendix Z) and full magnetization of the powerful magnetic structure may provide some difficulties.

Ray Newman

Ray Newman

APPENDIX X

ΔM DENOTES THE CHANGE IN MAGNET VOLUME FROM A OH TO UH SWITCH WITH NO CHANGE OF MAGNET MATERIAL TYPE AND COIL LENGTH ADJUSTED FOR SAME X_{MAX}.

ΔM′ IS A "MAGNET EQUIVALENT" QUANTITY ASSOCIATED WITH A SWITCH IN MAGNET MATERIAL TYPE WITH A "C" VALUE (TYPICALLY) BELOW .7 (SEE TEXT).

$$\Delta M \text{ OR } \Delta M' = \left(1 - 4\left[\frac{X_{GM}}{K_{OH}}\right]^2\right) \times \left(\frac{G_{OH} + 2X_{GM}}{G_{OH} + \frac{X_{GM}}{.5 - f}}\right) \times LF$$

TERM "A" TERM "B" TERM "C"

f IS AMOUNT OF COIL ALLOWED TO LEAVE GAP (¼, ½ ETC.)

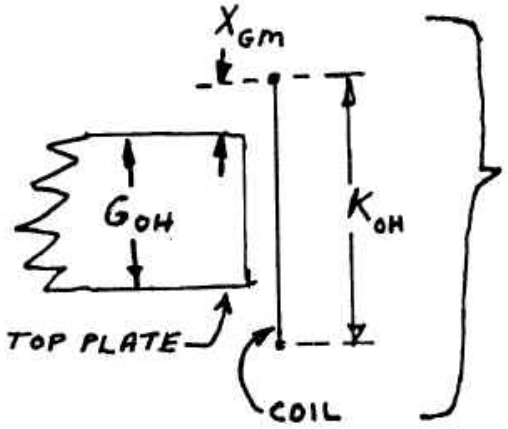

OVERHUNG COIL CASE THAT EQUATION IS BASED UPON

NOTE THAT THE UH TOP PLATE THICKNESS IS GIVEN BY $G_{UH} = G_{OH} + 4X_{GM}$

APPENDIX Y

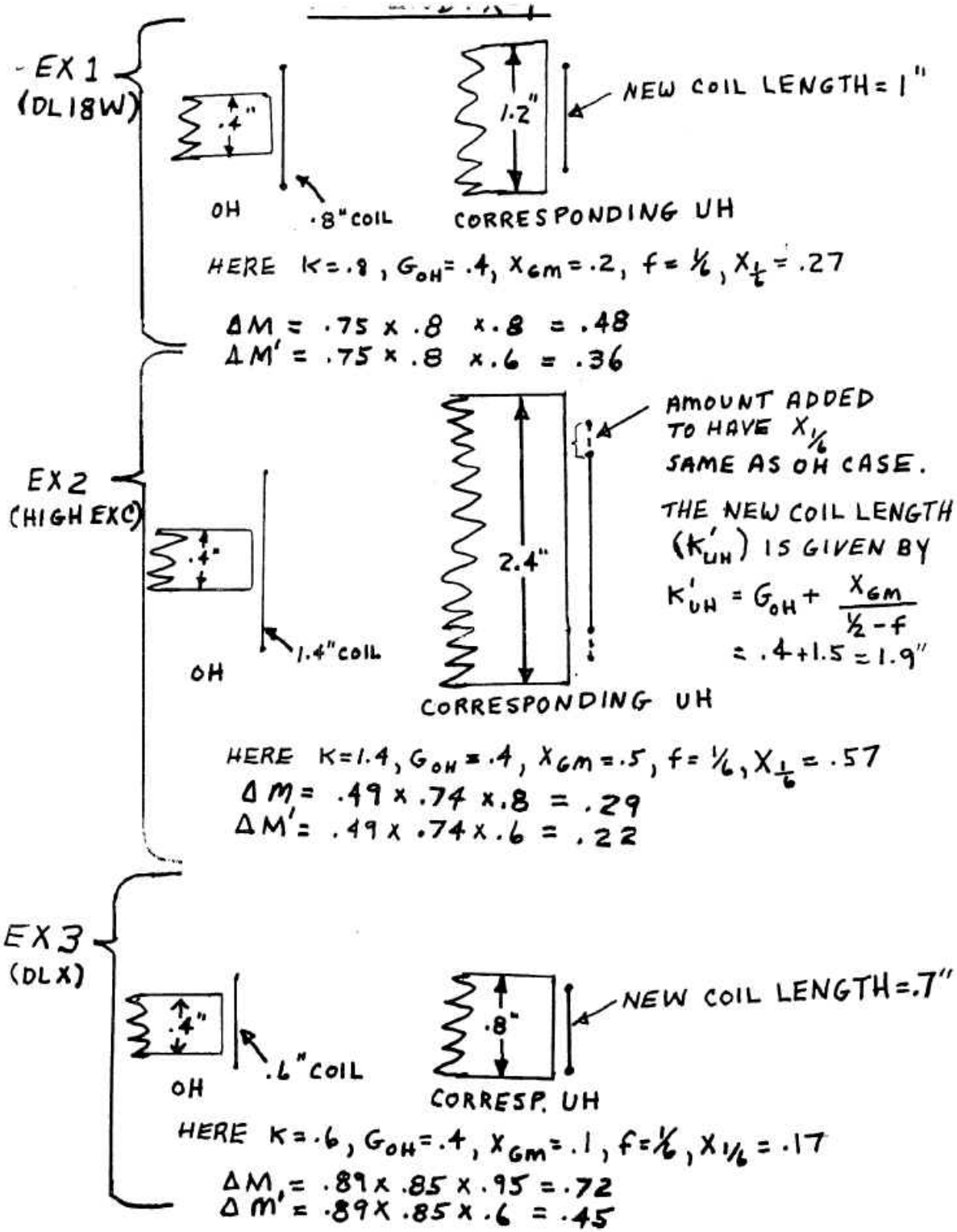
EX 1
(DL18W)
.4"
.8" COIL
OH
1.2"
NEW COIL LENGTH = 1"
CORRESPONDING UH
HERE K=.8, G_{OH}=.4, X_{GM}=.2, f=1/6, $X_{1/6}$=.27
ΔM = .75 x .8 x .8 = .48
ΔM' = .75 x .8 x .6 = .36
EX 2
(HIGH EXC)
.4"
1.4" COIL
OH
2.4"
AMOUNT ADDED TO HAVE $X_{1/6}$ SAME AS OH CASE.
THE NEW COIL LENGTH (K'_{UH}) IS GIVEN BY
$K'_{UH} = G_{OH} + \frac{X_{GM}}{1/2 - f}$
= .4+1.5 = 1.9"
CORRESPONDING UH
HERE K=1.4, G_{OH}=.4, X_{GM}=.5, f=1/6, $X_{1/6}$=.57
ΔM = .49 x .74 x .8 = .29
ΔM' = .49 x .74 x .6 = .22
EX 3
(DLX)
.4"
.6" COIL
OH
.8"
NEW COIL LENGTH = .7"
CORRESP. UH
HERE K=.6, G_{OH}=.4, X_{GM}=.1, f=1/6, $X_{1/6}$=.17
ΔM = .89 x .85 x .95 = .72
ΔM' = .89 x .85 x .6 = .45

APPENDIX Z

$\Delta\phi$ DENOTES THE CHANGE IN MAGNET SYSTEM TOTAL FLUX IN GOING FROM OH TO UH. (NOTATION DEFINED IN APPENDIX-X)

$$\Delta\phi = \left(\frac{K_{OH} + 2X_{Gm}}{K_{OH} - 2X_{Gm}}\right)^{1/2} \times \left(1 - 4\left[\frac{X_{Gm}}{K_{OH}}\right]^2\right)^{1/2} \times \left(\frac{G_{OH} + 2X_{Gm}}{G_{OH} + \frac{X_{Gm}}{.5 - F}}\right)^{1/2}$$

LOOKING AT APPENDIX-X, WE SEE THAT THIS IS IN THE FORM OF:

$$\Delta\phi = \left(\frac{K_{OH} + 2X_{Gm}}{K_{OH} - 2X_{Gm}}\right)^{1/2} \times A^{1/2} \times B^{1/2}$$

LOOKING AT APPENDIX-Y EXAMPLES:

$\Delta\phi$ (EX1) = 1.34

$\Delta\phi$ (EX2) = 1.47

$\Delta\phi$ (EX3) = 1.22

8. APPENDIX 2: AUTHOR'S REMINISCENCES

8.1. Don Keele's Reminiscences about Ray Newman

Credit Where Credit is Due.

One day in the lab, Ray took an un-mounted woofer into EV's large anechoic chamber and placed it on its back on the screened floor of the chamber. He placed the test B&K mic close to the center of the woofer's dust cap and went out of the chamber and then ran two SPL frequency responses using the B&K swept sine-wave signal generator and graphic level recorder. He gazed at the response curves for a short period of time and then quickly stated that the driver had a free-air resonance of 37 Hz, a total Q of 0.7 and a mechanical Q of 2.5. These were some of the then-new Thiele-Small parameters of the driver.

I thought it was magic at the time! He hadn't run any impedance curves or made any complicated Thiele-Small computations to determine the parameters. How had he done it?

Traditionally, the Thiele/Small driver parameters are fairly difficult to measure. The procedure usually requires running a detailed high-resolution impedance curve followed by several detailed calculations.

What I didn't know at the time that he was making a nearfield measurement of the un-mounted driver and then determining the Thiele-Small driver parameters by looking at a constant-voltage and a constant-current drive frequency response measurement. It's simple to determine by inspection the corner frequency and Q of a simple second-order high-pass filter that the near-field frequency response of the speaker approximates.

I thought the technique of placing the microphone close to the cone and measuring a response curve to determine low-frequency response was a technique worthy of investigation. I ended up with all the credit for the nearfield technique because I wrote a paper analyzing the technique that Ray was too busy to be included as co-author at the time. He should have gotten most of the credit!

8.2. David Carlson's Reminiscences about Ray Newman

Ray Newman had a passion for loudspeakers. My first contact with Ray was when I was a student in college and I contacted Electro-Voice to figure out how best to use some loudspeakers for a research project. At the time, I was impressed at how much interest he had in what I was doing. Ten years later, when I went to work for Ray, I got to witness that enthusiasm first hand.

Working with Ray was like working in a university environment. He was always interested in exploring new ideas or new ways to employ existing ideas. (This woofer paper is an example of that.) Besides working on new product development, he always encouraged me to set aside some time for what he called "Blue Sky Research". Over the years, we had many conversations in his office that would start out with "What would happen if we tried this"? It didn't matter if the idea was his or mine or something that grew out of the conversation - he was always excited to talk about the new ideas. It is remarkable to look back at how many of those "What if" discussions turned into real products.

Several decades have passed since the first of those conversations with Ray, but I can recall them as if they happened last week. Although Ray has been gone for some time now, his spirit continues to serve as a mentor.

8.3. Jim Long's Reminiscences about Ray Newman

Ray came to Electro-Voice loudspeaker engineering in Buchanan, Michigan, from the eastern part of the state, having engineered radar systems for military use. We were both in our late 20's. He told me that he would rather help make music than war. It wasn't long before we became very good friends. Although I was no longer working in EV engineering, we found we had a life-long interest in music and its quality reproduction, fine food and Calvados—introduced to us a bit later by a member of the French audio press.

The pipe organ was perhaps Ray's favorite musical instrument. He had the parts for a small one in his last home, but the organ itself never got put together. He did have an electronic organ in his home and I recall that he taught himself to play a short passage from one of the Widor organ sonatas, in hopes of gaining access to the organ that Widor himself had

played in Paris. Red tape precluded this French connection from working out.

Over the years, once every week or so, Ray and I would retire to his home (closer to work than mine) where he would make us lunch. Often pasta with a quickly made but delicious sauce of stewed tomatoes enhanced with sautéed garlic. Lunch was always accompanied by a glass of red wine, maybe two. We had so many lunches of this type from the late 1960's to just before he died in 1996 that they sometimes seem to be one big, fine lunch.

While at EV, Ray made at least two very important contributions to loudspeakers. I will never forget him walking into my office one morning with a copy of the May 1971 *Journal of the Audio Engineering Society* in his hand. He laid it on the table and said, "We need to pay attention to this." He was talking about the first of two papers by Australian A. N. Thiele describing a mathematical approach to vented loudspeakers based on electrical filter theory. He immersed himself in the math and all of the Thiele "alignments." He was entranced by what we came to call "the vented advantage," i.e., for a given box size one could select a calculable amount of increased efficiency or low-frequency extension or some combination of the two. Vented loudspeakers are now ubiquitous, which I attribute to Ray's interest in Thiele's work.

One of the outcomes of his fascination was a smaller-than-usual (22 in. x 14 in. x 7.75 in. hwd) "bookshelf" home high-fidelity loudspeaker called the Interface:A. It was at once a few dB more sensitive than the typical "acoustic suspension" sealed system of the day and made it all the way down to 32 Hz, 3 dB down, which intrigued Ray because it was great for pipe organs. The physical and acoustic parameters of the Interface:A were made possible by the so-called B_6 Thiele alignment. This alignment traded a box half the size for reduced very-low-frequency efficiency, getting flat response back with an underdamped high-pass filter providing a 6-dB boost at the box-tuning frequency of 32 Hz. So the speaker came with an active line-level equalizer to be inserted between preamp and power amp, pretty weird stuff for the mid 1970's. In the field, it was fun demonstrating how the roll-off below box tuning of the B_6 EQ served as a nice infrasonic filter, keeping LP record warp from wasting woofer cone motion (remember, this was before the compact disc). Four Interface:A's are still pumping away in my home theater system.

Along with his boss, John Gilliom, Ray also was very much involved in the concept of "constant directivity" as applied to horns for professional sound use. Constant directivity is taken for granted today, but not in the 1970's. Ray tinkered first with this in the horizontal plane, mocking up a tweeter based on the ancient EV T35 but with an entirely new horn and phase plug. This tweeter came to be called the T350 and embodied two of the three basic principles of constant directivity: conical (straight) horn side walls and a throat opening very small compared to the shortest wavelengths of interest, so that diaphragm output would be diffracted into the full 120° of the horn.

Don Keele came to EV around this time and ended up measuring the beamwidth versus frequency of the typical multicell and radial horns of the day. This was found to be highly variable. Don took the ideas from Ray and John, added important ones of his own, and produced the first line of constant-directivity horns, the EV HR "white horns" (so named because of their white fiberglass construction). Two of these horns are the backbone of my home stereo, along with custom LF horns and vented subs that Ray designed after he retired in 1993. More importantly, these first constant-directivity horns got Electro-Voice into the "pro sound" business.

I frequently think of Ray when I contemplate the home stereo and theater systems, fine food and fine friends.

Jim Long, Telex/EV

July 26, 2006

Ray Newman's circa-1971. ST350 horn tweeter prototype.

Jim Long and Don Keele in Jim's living room standing on either side of the right-channel HR-9040 "constant directivity" horn mounted over the bass horn designed by Ray Newman. Sept. 2004.

8.4. Matt Ruhlen's Reminiscences about Ray Newman

The Blooming Sansevieria Trifasciata Plant[2]

Ray Newman was my boss while I worked at Electro-Voice. More notably, Ray was a friend & mentor. He was not your typical loudspeaker engineer; rather, he was full of whimsical insight into life.

Ray would offer advice to problems in the form of questions, letting you walk the path to answer your own in your words.

In a 1988 magazine interview Ray was asked, "Where would loudspeaker technology be in five years?" Rather than giving specific details about up-incoming gadgets, Ray explained that the industry needed to listen to its customers and present solutions to their problems. Those solutions would lead the industry to the next level of loudspeaker technology.

This was Ray.

Ray had an artistic side that most didn't know. Poetry and photography were just a few of his favorite non-engineering past times. Ray would make his own Christmas cards by taping pictures to pieces of folded paper and using a typewriter to include poetry on the inside, then photocopy them. The first time I saw him making his Christmas cards I thought he was being, well, cheap. But after I got one of his cards, the simplistic function and meaning of the message contained was all a part of the "photocopying".

All loudspeaker system designs are interrelated and draw from certain basic scientific principles with art.

---

[2] Definition from Wikipedia:
Sansevieria trifasciata is a species of Sansevieria, native to tropical west Africa from Nigeria east to the Democratic Republic of the Congo. It is commonly called the snake plant, because of the shape of its leaves, or mother-in-law's tongue because of their sharpness.

It is an evergreen herbaceous perennial plant forming dense stands, spreading by way of its creeping rhizome, which is sometimes above ground, sometimes underground. Its stiff leaves grow vertically from a basal rosette. Mature leaves are dark green with light gray-green cross-banding and usually range between 70–90 cm in length and 5–6 cm in width.

The emphasis placed on the principles changes depending on the specific market they serve. -Plato- (Ray Newman)

This was Ray.

To the AES community, a Preprint (#2342) with the title "Do you Have Sufficient Quantity of Acoustic Benzene?" might seem a little unusual. After you get past the title, aside from an enlightening technical paper about cone excursions, you will also find a reference to "Darwinian process" and "running out of benzene while driving".

This was Ray.

The day Ray left Electro-Voice, he gave me the plant that sat on his desk. This plant, whose flowers are a rare sight, is fittingly, a part of Ray. Over the years, his plant has grown, but just about the time Don Keele started working on Ray's memo, the plant (a Mother-in-law's Tongue; Sansevieria trifaciata) bloomed for the first time, perhaps as Ray's words will soon bloom.

A Sansevieria Trifasciata Plant

(Photo courtesy Wikipedia)

A Sansevieria Trifasciata plant in flower

(Photo courtesy Wikipedia)